ChemPubSoc Europe

DOI: 10.1002/cmdc.201700044

CHEMMEDCHEM Full Papers

VIP *Very Important Paper*

Novel Pieces for the Emerging Picture of Sulfoximines in Drug Discovery: Synthesis and Evaluation of Sulfoximine Analogues of Marketed Drugs and Advanced Clinical Candidates

Juan Alberto Sirvent and Ulrich Lücking*[a]

Sulfoximines have gained considerable recognition as an important structural motif in drug discovery of late. In particular, the clinical kinase inhibitors for the treatment of cancer, roniciclib (pan-CDK inhibitor), BAY 1143572 (P-TEFb inhibitor), and AZD 6738 (ATR inhibitor), have recently drawn considerable attention. Whilst the interest in this underrepresented functional group in drug discovery is clearly on the rise, there remains an incomplete understanding of the medicinal-chemistry-relevant properties of sulfoximines. Herein we report the synthesis and in vitro characterization of a variety of sulfoximine analogues of marketed drugs and advanced clinical candidates to gain a better understanding of this neglected functional group and its potential in drug discovery.

Introduction

Since the late discovery of the first sulfoximine compound in 1949,[1] sulfoximine chemistry[2] has been a rather niche discipline, explored by only a few research groups worldwide. Applications have mainly centered around the use of sulfoximines as either chiral auxiliaries[3] or ligands in asymmetric catalysis.[4] Satzinger and Stoss at Gödecke AG pioneered the use of the sulfoximine group in medicinal chemistry in the 1970s.[5] However, until very recently, the sulfoximine group has rarely been employed in drug discovery applications, even though it offers a unique combination of interesting properties, namely high chemical and metabolic stability, favorable physicochemical properties, hydrogen-bond acceptor/donor functionalities, and structural diversity.[6] To date, there is no approved drug containing a sulfoximine group and the number of sulfoximine compounds evaluated in clinical trials has been very limited. A similar picture has emerged in crop protection applications; however, use of the sulfoximine insecticide sulfoxaflor was approved in 2013.[7]

Low commercial availability and limited available synthetic methods with associated safety concerns[8] have likely hindered the use of the sulfoximine group historically, especially in industry. However, over the last decade, activity in sulfoximine chemistry has increased considerably, leading to new and safe synthetic methods.[9] Developments of late include, for instance, the use of flow chemistry techniques,[10] the palladium-catalyzed direct α-arylation of protected *S*,*S*-dimethylsulfoximine,[11] and the first method for the direct synthesis of NH-sulfoximines from sulfides.[12] This progress in synthetic methodology has coincided with the rapidly increasing interest in sulfoximines as pharmacophores in the life sciences.[13] In drug discovery, the clinical kinase inhibitors for the treatment of cancer, roniciclib,[13b,14] BAY 1143572,[15] and AZD 6738,[16] have been the focus of considerable attention recently (Figure 1).

Even though the interest was rather limited for many decades, research has been conducted in which the sulfoximine group was used in opportunistic approaches to replace a surprising variety of functional groups including alcohol, acid, amidine, sulfone, and sulfonamide moieties.[6] Very recently, the physicochemical properties and behavior in selected in vitro assays of a set of small and fragment-like sulfoximines in comparison with related sulfur-based analogues and amides has been reported.[17] To overcome the limitations of analyzing such small and fragment-like compounds, that study also contained a matched molecular pair analysis of sulfoximines and related compounds from drug discovery projects at Boehringer Ingelheim. However, this qualitative analysis did not disclose the corresponding chemical structures and assay data.

During the course of our long-standing interest in sulfoximines as an underrepresented pharmacophore in drug discovery,[18] we have investigated a variety of approaches which were not intended to identify clinical candidates but to improve our general understanding of the sulfoximine functional group with respect to synthesis[11] and medicinal chemistry relevant properties. One idea was to synthesize direct sulfoximine analogues of marketed drugs or advanced clinical candidates to compare the in vitro properties of the matched molecular pairs. Our selection of the corresponding target molecules was mainly triggered by synthetic opportunity, our general interest

[a] *Dr. J. A. Sirvent, Dr. U. Lücking*
Drug Discovery, Bayer AG, Müllerstr. 178, 13353 Berlin (Germany)
E-mail: ulrich.luecking@bayer.com

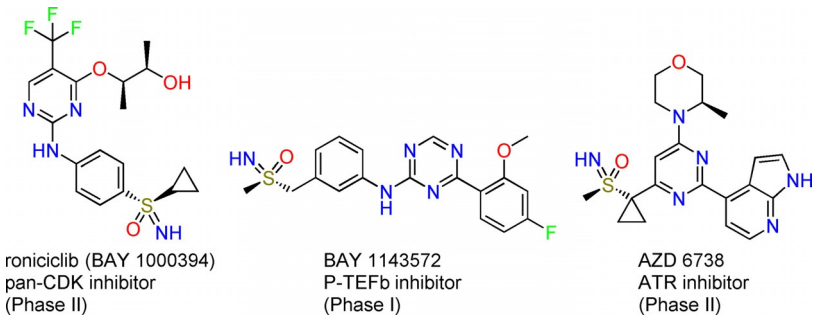

Figure 1. Structures of clinical kinase inhibitors roniciclib, BAY 1143572, and AZD 6738 for the treatment of cancer.

in kinase inhibitors, and/or the possibility of evaluating the test compounds in readily available assays. Moreover, we were also interested in investigating the effects of the replacement of non-sulfur-based functional groups, such as amines which are ubiquitous in life science approaches, by sulfoximines. Herein, we report the synthesis and in vitro characterization of six sulfoximine analogues of marketed drugs (imatinib, palbociclib, vardenafil, fulvestrant) and advanced clinical candidates (AT7519, ribociclib).

Results and Discussion

Imatinib

Deregulated protein tyrosine kinase activity is central to the pathogenesis of human cancers. Targeted therapy in the form of selective tyrosine kinase inhibitors has transformed the approach for the management of various cancers and represents a therapeutic breakthrough. Imatinib mesylate, an oral small-molecule inhibitor of several tyrosine kinases, including ABL, KIT, and PDGFR, was one of the first cancer therapies to show the potential for such targeted action.[19] Imatinib, the standard of care in chronic myelogenous leukemia and certain gastrointestinal stromal tumors, has dramatically changed the outlook of patients affected by these diseases.

The chemical structure of imatinib contains a polar side chain, an *N*-methylpiperazinyl moiety (Figure 2), that markedly improves both solubility and oral bioavailability.[20] Under physiological conditions, the piperazinyl group is predominantly protonated and imatinib carries a net positive charge in the bound complex with tyrosine kinases. This enables hydrogen-bonding interactions between imatinib and the backbone carbonyl of specific residues in the binding pocket.[21] Moreover, imatinib is primarily metabolized at the *N*-methylpiperazinyl moiety to an active metabolite, the *N*-demethylated piperazine derivative.[22]

The introduction of water-solubilizing groups, such as morpholinyl, piperazinyl, piperidinyl, and acyclic tertiary amino, at positions that project toward solvent, and therefore do not compromise inhibitory potency, is a common approach for improving the physicochemical properties of kinase inhibitors.[23] However, the introduction of basic solubilizing groups can also greatly affect ADME properties such as permeability, metabolic stability, absorption, clearance, oral bioavailability, and target organ exposure. It also bears a number of risks with respect to toxicity, including higher affinity for hERG channels with associated risks of QT prolongation, induction of phospholipidosis, and/or potential for increased off-target activity.[24]

In an opportunistic approach, we wondered if 1λ^6-thiomorpholine-1-imine 1-oxide could serve as a structural alternative for the *N*-methylpiperazine group[25] in imatinib, originally incorporated into the molecule to improve solubility. Like the protonated *N*-methylpiperazine group, the sulfoximine group is tetrahedral and has been described as offering favorable physicochemistry in conjunction with good DMPK properties. Moreover, the sulfoximine group has dual hydrogen-bond donor/acceptor functionality, but significantly decreased basicity.[6,17]

The required sulfoximine building block **4** was synthesized in four steps from thiomorpholine. Thus, the amino group was first conveniently protected by reaction with benzyl chloroformate (CbzCl). Then, oxidation of the resulting sulfide **1** to sulfoxide **2**, followed by rhodium-catalyzed imination with 2,2,2-trifluoroacetamide,[9a] afforded sulfoximine **3**, which was finally

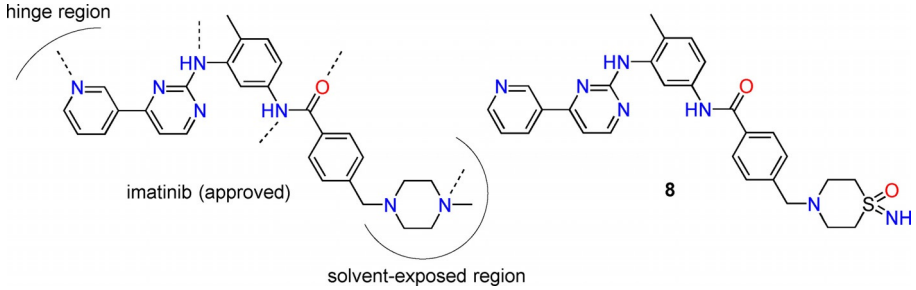

Figure 2. Structure of imatinib with its proposed binding mode to tyrosine kinase,[26] and structure of sulfoximine analogue **8**.

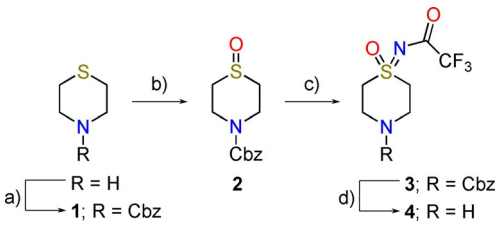

Scheme 1. Synthesis of building block **4**. *Reagents and conditions*: a) CbzCl, NaOH (aq. 1 M), 0 °C→RT, 3 h, 98%; b) H_5IO_6 (1.1 equiv), $FeCl_3$ (3 mol%), MeCN, RT, 3 h, crude; c) $H_2NC(O)CF_3$ (2 equiv), $Rh_2(OAc)_4$ (2.5 mol%), MgO (4 equiv), $PhI(OAc)_2$ (1.5 equiv), CH_2Cl_2, RT, 20 h, 45%; d) H_2 (1 atm), Pd/C (10 wt%), MeOH, RT, 5 h, crude.

subjected to hydrogenolysis to remove the Cbz group (Scheme 1).

The amide partner **6** was then prepared in quantitative yield by coupling of the commercial building block **5** and 4-(chloromethyl)benzoyl chloride (Scheme 2). Subsequent reaction of benzyl chloride **6** with amine **4**, followed by removal of the trifluorocarbonyl group attached to the sulfoximine nitrogen in **7** under basic conditions, afforded the desired imatinib sulfoximine analogue **8**.

Relative to the reported quantitative dissociation constants (K_d) of imatinib,[27] sulfoximine analogue **8** exhibited reduced binding to non-phosphorylated ABL1 (imatinib K_d = 1.1 nM vs. **8** K_d = 79 nM). However, potent in vitro binding of analogue **8** to KIT (K_d = 11 nM) and PDGFRβ (K_d = 19 nM) was recorded, very similar to the reported data for imatinib (KIT K_d = 13 nM, PDGFRβ K_d = 14 nM) (Table 1). This modulated selectivity profile of analogue **8** is quite surprising, since the sulfoximine group of the bound inhibitor is also expected to be directed toward the exit of the ATP binding pocket.

Aqueous solubility (S_w) of both compounds at pH 6.5 was determined by an orienting, high-throughput screening method using 1 mM DMSO stock solutions.[28] Imatinib has an aqueous solubility of 112 mg L^{-1}, compared with 54 mg L^{-1} for analogue **8**. Similar log*D* values at pH 7.5 for imatinib (1.9) and for analogue **8** (2.0) were recorded by using a method for determining hydrophobicity constants by reversed-phase HPLC[29] (Table 1).

In vitro pharmacokinetic studies with imatinib and sulfoximine analogue **8** revealed a trend for a slightly improved metabolic stability of **8** in rat hepatocytes, resulting in a moderate predicted blood clearance (CL_b) of 1.9 L h^{-1} kg^{-1} for sulfoximine **8**, compared with 2.3 L h^{-1} kg^{-1} for imatinib. Similar observations were made with human liver microsomes (CL_b of 0.34 L h^{-1} kg^{-1} for **8** vs. 0.48 L h^{-1} kg^{-1} for imatinib). However, in the Caco2 screening assay, analogue **8** had a significantly decreased permeability coefficient (P_{app} A→B) of < 2 nm s^{-1} and a high efflux ratio of > 134, compared with imatinib with a moderate permeability coefficient (P_{app} A→B) of 39 nm s^{-1} and a moderate efflux ratio of 2.7 (Table 1).

With rather similar solubility at pH 6.5, as determined in the high-throughput screening method, and very similar log*D* value, the pronounced decrease in permeability and increased efflux ratio of sulfoximine analogue **8** relative to imatinib is surprising. The structural change from the *N*-methylpiperazine group to the 1λ⁶-thiomorpholine-1-imine 1-oxide analogue results in an increased topological polar surface area (TPSA) and molecular weight (see Table 6 below). An additional hydrogen-bond donor is also introduced. Nevertheless, the TPSA of 123.96 and the number of hydrogen-bond donors (three) and acceptors (eight) of analogue **8** is still within most of the generally accepted drug-like score rules.[31] Only its molecular

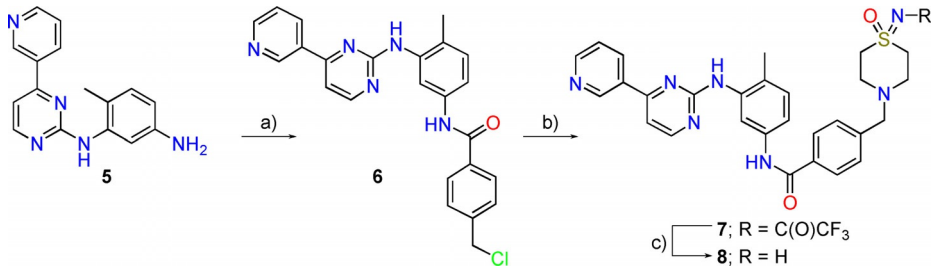

Scheme 2. Synthesis of imatinib analogue **8**. *Reagents and conditions*: a) 4-(chloromethyl)benzoyl chloride (1.1 equiv), K_2CO_3 (2.1 equiv), THF, 0 °C, 2 h, then RT, 2 h, 99%; b) **4** (1.5 equiv), Et_3N (2 equiv), DMF, 150 °C, 24 h; c) K_2CO_3 (2 equiv), MeOH, RT, 1 h, 5% (2 steps).

Table 1. Comparison of the in vitro properties of imatinib and sulfoximine analogue **8**.

Compd	K_d [nM]			S_w pH 6.5 [mg L^{-1}][c]	log*D* pH 7.5[d]	CL_b [L h^{-1} kg^{-1}][e]		P_{app} A→B [nm s^{-1}][f]	ER[f]
	ABL1	KIT	PDGFRβ			rHep	hLMs		
imatinib	1.1[a]	13[a]	14[a]	112	1.9	2.3	0.48	39	2.7
8	79[b]	11[b]	19[b]	54	2.0	1.9	0.34	< 2	> 134

[a] Reported K_d values of imatinib,[27] determined by KINOMEscan® Profiling Service, DiscoverX. [b] Determined by KINOMEscan® Profiling Service, DiscoverX. [c] Determined by a high-throughput screening method using 1 mM DMSO stock solutions.[28] [d] Determined by reversed-phase HPLC.[29] [e] Predicted hepatic metabolic clearance based on a high-throughput metabolic stability assay using 1) freshly harvested rat hepatocytes (rHep) and 2) pooled human liver microsomes (hLMs).[30] [f] P_{app} A→B (apical to basolateral) and efflux ratio (ER) data were generated in a bidirectionally performed Caco2 permeability assay in a 24-well format; ER was calculated as P_{app} B→A/P_{app} A→B.[30]

weight of 527.64 Dalton is slightly above the rule of five;[32] however, according to a recent analysis, >30% of approved small-molecule kinase inhibitors have a molecular weight exceeding 500.[33]

Pan-CDK inhibitor AT7519

Cyclin-dependent kinases (CDKs) belong to a family of serine/threonine kinases which associate with an activating cyclin regulatory subunit. Cell-cycle kinases 1, 2, 4, and 6 are required for the correct timing and order of the events of the cell-division cycle, whereas non-cell-cycle CDKs 7 and 9 are involved in gene transcription via regulation of RNA polymerase II activity. Deregulated CDK activity results in the loss of function of cell-cycle checkpoints and increased expression of anti-apoptotic proteins, which have both been directly linked to the molecular pathology of cancer. Since their discovery, CDKs have been considered strong prospective targets for a new generation of anticancer drugs.[34]

AT7519 is a potent, small-molecule multi-CDK inhibitor that has been evaluated in clinical phase II trials[35] (Figure 3). AT7519 was discovered using fragment-based medicinal chemistry approaches, linked to high-throughput X-ray crystallography.[36] During lead optimization, introduction of the solubilizing aminopiperidine amide group resulted in improved selectivity for CDKs over other kinases, improved cellular activity, and lower plasma clearance. In the CDK2 co-crystal structure of AT7519, the piperidinyl moiety is pointing out of the ATP binding pocket, toward solvent.[37]

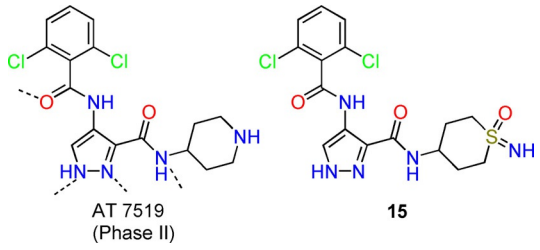

Figure 3. Structure of multi-CDK inhibitor AT7519 with its proposed binding mode to CDK2,[37] and structure of sulfoximine analogue **15**.

Along the lines of imatinib analogue **8**, the effects of a switch from the solubilizing 4-aminopiperidine group of AT7519 to the sulfoximine analogue **15** were investigated (Figure 3). The synthesis of analogue **15** involved initial preparation of the sulfoximine building block **12**, starting from tetrahydro-2*H*-thiopyran-4-amine (Scheme 3), via the same sequence of transformations as used for the synthesis of building block **4**. Then, amide coupling of amine **12** with commercial acid **13** in the presence of EDC and HOBt, followed by deprotection of sulfoximine **14** under basic conditions, afforded the desired compound **15**.

With an IC_{50} of 522 nM against CDK2 and of 124 nM against CDK9, sulfoximine analogue **15** exhibited decreased CDK inhibitory activity in vitro relative to AT7519, with an IC_{50} of 96 nM against CDK2 and of 6 nM against CDK9 (Table 2). Both compounds showed potent antiproliferative activity against A2780 cells in vitro. The higher biochemical potency of AT7519 translated into a higher antiproliferative potency against A2780 cells, with an IC_{50} of 131 nM, relative to an IC_{50} of 351 nM for analogue **15**.

The thermodynamic solubility of AT7519 and analogue **15** in water at pH 6.5 was determined by an equilibrium shake flask method.[38] AT7519 has a high aqueous solubility of 1524 mg L^{-1}, compared to 52 mg L^{-1} for sulfoximine **15**. Using reversed-phase HPLC, a slightly increased log*D* value of 1.6 at pH 7.5 for analogue **15** was recorded, compared to 1.3 for AT7519 (Table 2).

Sulfoximine analogue **15** displayed a significantly improved in vitro metabolic stability in rat hepatocytes with a low predicted CL_b of 0.06 L h^{-1} kg^{-1}, compared to a moderate predicted CL_b of 1.7 L h^{-1} kg^{-1} for AT7519. A similar trend was observed with human liver microsomes (CL_b of 0.06 L h^{-1} kg^{-1} for **15** vs. 0.24 L h^{-1} kg^{-1} for AT7519; Table 2). Interestingly, both compounds have a very low permeability coefficient (P_{app} A→B) of <2 nm s^{-1} and a high efflux ratio, even though their mo-

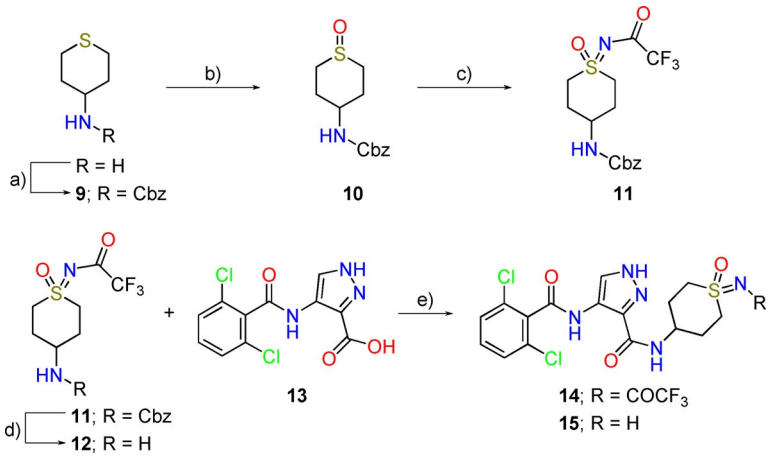

Scheme 3. Synthesis of AT7519 analogue **15**. *Reagents and conditions*: a) CbzCl (1.0 equiv), NaOH (aq. 1.0 M), 5 °C→RT, 1 h, 58%; b) H_5IO_6 (1.06 equiv), $FeCl_3$ (2.8 mol%), MeCN, RT, 3 h, 99%; c) $H_2NC(O)CF_3$ (2 equiv), $Rh_2(OAc)_4$ (5 mol%), MgO (4 equiv), $PhI(OAc)_2$ (1.5 equiv), CH_2Cl_2, RT, 72 h, 35%; d) H_2 (1 atm), Pd/C (10 wt% Pd), MeOH, RT, 5 h, crude; e) EDC (1.2 equiv), HOBt (1.2 equiv), DMF, RT, 42 h, **14** (12%) and **15** (20%).

Table 2. Comparison of the in vitro properties of AT7519 and sulfoximine analogue **15**.

Compd	IC_{50} [nM] CDK2[a]	CDK9[a]	A2780[b]	S_w pH 6.5 [mg L^{-1}][c]	log*D* pH 7.5[d]	CL_b [L h^{-1} kg^{-1}][e] rHep	hLMs	P_{app} A→B [nm s^{-1}][f]	ER[f]
AT7519	96	6	131	1524	1.3	1.7	0.24	1.0	92
15	522	124	351	52	1.6	0.06	0.06	1.4	37

[a] IC_{50} values determined in biochemical in vitro kinase assays in the presence of 10 μM ATP.[39] [b] IC_{50} values determined in an in vitro proliferation assay using cultivated A2780 cells.[39] [c] Thermodynamic solubility in water determined by an equilibrium shake flask method;[39] solid state of the test compounds was not characterized. [d] Determined by reversed-phase HPLC.[29] [e] Predicted hepatic metabolic clearance based on a high-throughput metabolic stability assay using 1) freshly harvested rat hepatocytes (rHep) and 2) pooled human liver microsomes (hLMs).[30] [f] P_{app} A→B (apical to basolateral) and efflux ratio (ER) data were generated in a bidirectionally performed Caco2 permeability assay in a 24-well format; ER was calculated as P_{app} B→A/P_{app} A→B.[30]

lecular weight, TPSA, and number of hydrogen-bond donors/acceptors are not critical according to most of the generally accepted drug-like score rules[31] (see Table 6).

Selective CDK4/6 inhibitors palbociclib and ribociclib

Numerous pharmaceutical companies have initiated drug discovery efforts to identify low-molecular-weight CDK inhibitors for cancer therapy, but most pan-CDK inhibitors have failed rigorous clinical testing so far, at least in part because nonselective pan-CDK inhibition is toxic to noncancerous cells.[40] These issues of effectiveness and toxicity seem to have been overcome by the more selective targeting of CDK4 and CDK6, a pair of kinases that are similar in structure and function, which mediate transition from the G_0/G_1-phase to the S-phase of the cell cycle. Three of these new CDK4/6 inhibitors (abemaciclib, palbociclib, and ribociclib) have emerged, following the findings of early phase trials, as agents with promising anticancer activity and manageable toxicity.[41] Palbociclib received accelerated FDA approval in 2015, in the setting of hormone receptor (HR) positive, advanced-stage breast cancer. In 2016, ribociclib received FDA breakthrough therapy designation as the first-line treatment for HR+/HER2− advanced breast cancer.

The 2-aminopyrido[2,3-*d*]pyrimidin-7-one core of palbociclib (Figure 4) forms two hydrogen bonds to the kinase hinge region via the pyrimidine N3 nitrogen and the exocyclic 2-amino group.[42] Two additional hydrogen bonds, via the pyridine nitrogen of the pyridylamino side chain and the acetyl group, orientate the inhibitor in the ATP binding pocket. The piperazine group of the C2 side chain of palbociclib is directed toward the exit of this ATP binding pocket. Replacing the piperazine group by a variety of heterocyclic groups resulted in little effect on the binding affinity,[42b] suggesting that the presence of a bulky group at this position improves inhibitor potency but contributes little to kinase selectivity. As a result of lead optimization to palbociclib, the piperazinyl substituent of the C2 side chain was considered optimal with regard to potency and physical properties. This structural motif is also found in ribociclib[43] and, in the form of the ethyl analogue, in abemaciclib.[44]

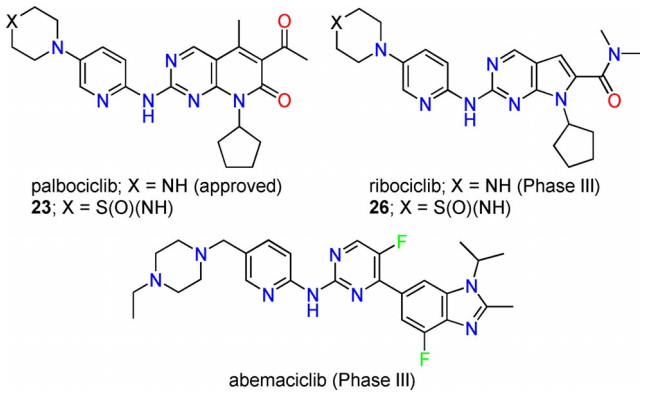

Figure 4. Structures of selective CDK4/6 inhibitors palbociclib, ribociclib, and abemaciclib, and of sulfoximine analogues **23** and **26**.

Along the lines of imatinib analogue **8**, the effects of a switch from the bulky, solubilizing piperazine group of palbociclib and ribociclib to the corresponding sulfoximine analogues **23** and **26** were investigated (Figure 4).[45] The sulfoximine analogues of palbociclib and ribociclib were both synthesized using the Boc-protected sulfoximine building block **19** (Scheme 4). The synthesis of **19** was accomplished in four

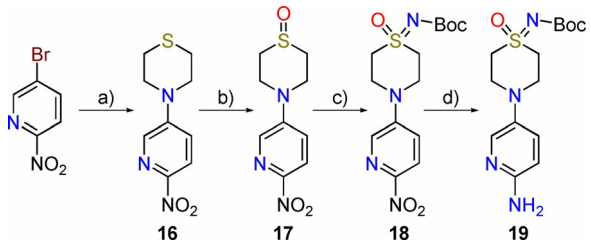

Scheme 4. Synthesis of building block **19**. *Reagents and conditions*: a) thiomorpholine (1.5 equiv), neat, 120 °C, 1 h, 99%; b) H_2O_2 (aq. 30%), RT, 4 h, 62%; c) $H_2NCOOtBu$ (1.5 equiv), $Rh_2(OAc)_4$ (2.5 mol%), MgO (4 equiv), $PhI(OAc)_2$ (1.5 equiv), DCE, 40 °C, 5 h, 83%; d) H_2 (1 atm), Pd/C (10 wt% Pd, 0.1 equiv), EtOH, RT, 2 h, 68%.

steps starting from thiomorpholine and commercial 5-bromo-2-nitropyridine. Heating these two compounds at 120 °C for 1 h without solvent resulted in quantitative formation of the coupled product **16**. Sulfide oxidation to the corresponding sulfoxide **17** was carried out in good yield with aqueous H_2O_2, without sulfone formation. Direct rhodium-catalyzed imination of **17** with *tert*-butyl carbamate following the procedure described by Luisi, Bull, and co-workers[9j] gave the Boc-protected

sulfoximine **18** in 83% yield. Reduction of the nitro group by hydrogenolysis proceeded cleanly to provide the aminopyridine **19** in 68% yield.

The synthesis of palbociclib analogue **23** was then accomplished via the nucleophilic addition of building block **19** to the commercial chloropyrimidine **20**, which gave coupled product **21**. Subsequent Stille coupling with tributyl(1-ethoxyvinyl)tin followed by acid hydrolysis was used to introduce an acetyl group, forming precursor **22**, which finally was deprotected with TFA to provide the desired product **23** (Scheme 5).

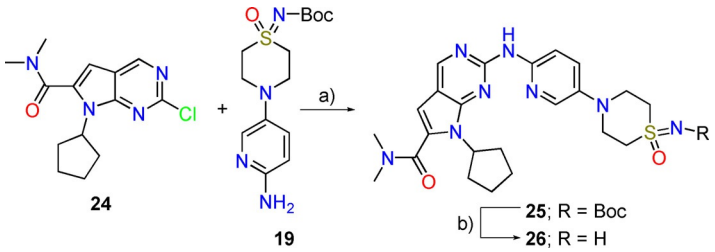

Scheme 6. Synthesis of ribociclib analogue **26**. *Reagents and conditions*: a) $Pd(OAc)_2$ (5 mol%), *rac*-BINAP (5 mol%), Cs_2CO_3 (1.4 equiv), dioxane, 110 °C, 6 h, 71%; b) TFA (7 equiv), CH_2Cl_2, RT, 5 h, 67%.

The synthesis of ribociclib analogue **26** was completed in two steps from building block **19**: palladium-catalyzed amination of commercial chloropyrimidine **24**, followed by cleavage of the *N*-Boc protecting group in coupled product **25** under acidic conditions, gave the desired sulfoximine **26** (Scheme 6).

In comparison with palbociclib, sulfoximine analogue **23** exhibited lower but more balanced inhibitory activity in vitro against CDK4 and CDK6 (Table 3). Palbociclib and its analogue **23** both showed potent antiproliferative activity against MOLM-13 cancer cells in vitro, with an IC_{50} of 41 nM and of 128 nM, respectively. Put side by side, ribociclib was more active than its sulfoximine analogue **26** against both CDK4 and CDK6. Interestingly, the difference in antiproliferative activity against MOLM-13 in vitro for the latter pair of compounds was quite pronounced, with an IC_{50} of 89 nM for ribociclib vs. 1150 nM for **26**.

The thermodynamic solubility of palbociclib and analogue **23** in water at pH 6.5, as determined by an equilibrium shake flask method,[38] is very similar (34 mg L^{-1} for palbociclib vs. 30 mg L^{-1} for **23**). Using reversed-phase HPLC,[29] a slightly increased log*D* value of 2.0 at pH 7.5 for analogue **23** was recorded, compared with 1.9 for palbociclib (Table 3). Relative to ribociclib, sulfoximine analogue **26** also exhibited a slightly increased log*D* value; however, the difference in thermodynamic, aqueous solubility at pH 6.5 proved to be more pronounced than the palbociclib matched pair, with 334 mg L^{-1} recorded for ribociclib vs. 22 mg L^{-1} for **26**.

In vitro pharmacokinetic studies with palbociclib and analogue **23** again revealed a trend for a slightly improved stability of the sulfoximine analogue in rat hepatocytes, resulting in a low predicted CL_b of 1.1 L h^{-1} kg^{-1} for sulfoximine **23**, compared with 1.3 L h^{-1} kg^{-1} for palbociclib. A similar trend was observed with human liver microsomes (Table 3). However, in the Caco2 screening assay, analogue **23** had a decreased permeability coefficient (P_{app} A→B) of 25 nm s^{-1} and an increased efflux ratio of 9.1, relative to palbociclib with a permeability co-

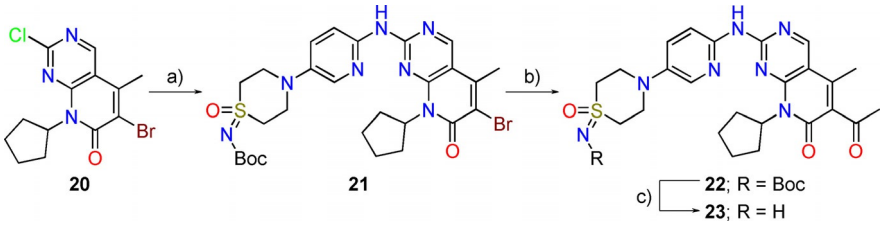

Scheme 5. Synthesis of palbociclib analogue **23**. *Reagents and conditions*: a) **19** (1 equiv), *i*PrMgCl (3.1 equiv), THF, 0 °C→RT, 21 h, 15%; b) tributyl(1-ethoxyvinyl)tin (1.5 equiv), $PdCl_2(PPh_3)_2$ (8.5 mol%), dioxane, 100 °C, 7 h, then HCl, RT, 2 h; c) TFA (7 equiv), CH_2Cl_2, 1 h, 64% (2 steps).

Table 3. Comparison of the in vitro properties of palbociclib and ribociclib, and their sulfoximine analogues **23** and **26**.

Compd	IC_{50} [nM] CDK4[a]	CDK6[a]	MOLM-13[b]	S_w pH 6.5 [mg L^{-1}][c]	log*D* pH 7.5[d]	CL_b [L h^{-1} kg^{-1}][e] rHep	hLMs	P_{app} A→B [nm s^{-1}][f]	ER[f]
palbociclib	7	57	41	34	1.9	1.3	0.45	70	2.6
23	101	240	128	30	2.0	1.1	0.24	25	9.1
ribociclib	67	803	89	334	1.7	2.3	0.52	135	1.3
26	216	>1000	1150	22	1.8	1.1	0.21	22	11

[a] IC_{50} values determined in biochemical assays at ProQinase, in the presence of 10 μM ATP (CDK4/CycD3) or 30 μM ATP (CDK6/CycD3). [b] IC_{50} values determined in an in vitro proliferation assay using MOLM-13 cells.[39] [c] Thermodynamic solubility in water determined by an equilibrium shake flask method;[39] solid state of the test compounds was not characterized. [d] Determined by reversed-phase HPLC.[29] [e] Predicted hepatic metabolic clearance based on a high-throughput metabolic stability assay using freshly harvested rat hepatocytes (rHep) and (ii) pooled human liver microsomes (hLMs).[30] [f] P_{app} A→B (apical to basolateral) and efflux ratio (ER) data were generated in a bidirectionally performed Caco2 permeability assay in a 24-well format; ER was calculated as P_{app} B→A/P_{app} A→B.[30]

efficient (P_{app} A→B) of 70 nm s^{-1} and an efflux ratio of 2.6. A low predicted CL_b of 1.1 L h^{-1} kg^{-1} was also recorded for sulfoximine analogue **26**, whereas ribociclib had a moderate CL_b of 2.3 L h^{-1} kg^{-1}. The trend for a higher in vitro metabolic stability of sulfoximine analogue **26** was also observed with human liver microsomes. Along the lines of the palbociclib/analogue **23** pair, sulfoximine **26** also had decreased permeability and an increased efflux ratio relative to ribociclib.

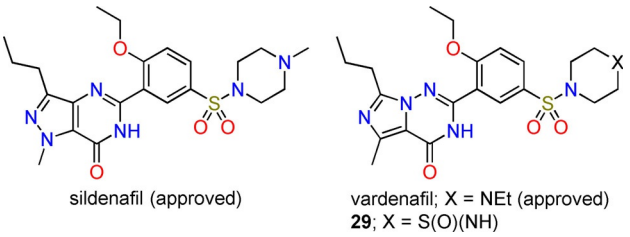

Figure 5. Structures of PDE5 inhibitors sildenafil and vardenafil, and of sulfoximine analogue **29**.

Vardenafil

Penile erection is a hemodynamic process initiated by the relaxation of smooth muscle in the corpus cavernosum and its associated arterioles. Nitric oxide, which is released from nerve endings and endothelial cells in the corpus cavernosum during sexual stimulation, activates the enzyme guanylate cyclase resulting in increased synthesis of cyclic guanosine monophosphate (cGMP) in the smooth muscle cells of the corpus cavernosum. cGMP in turn triggers smooth muscle relaxation, allowing increased blood flow into the penis, resulting in erection. The tissue concentration of cGMP is regulated by both the rates of synthesis and degradation via phosphodiesterases (PDEs). The most abundant PDE in the human corpus cavernosum is the cGMP-specific phosphodiesterase type 5 (PDE5); thus, the inhibition of PDE5 enhances erectile function by increasing the amount of cGMP.[46] For the treatment of erectile dysfunction, the differentiation of marketed PDE5 inhibitors based on efficacy is limited, whereas differentiation based on the pharmacokinetic profile (e.g., longer half-life and/or faster onset) is possible.[47] Because PDE5 is also present in the arterial wall smooth muscle within the lungs, the PDE5 inhibitors sildenafil and tadalafil are also FDA-approved for the treatment of pulmonary hypertension.

Sildenafil, the prototypical PDE5 inhibitor (Figure 5), binds to the active site of PDE5 by a combination of hydrophobic and polar interactions, in which the hydrophobic interactions dominate.[48] The pyrimidinone –NHCO– fragment forms a dual hydrogen bond, while the pyrazole *N*-methyl group fills a small hydrophobic pocket, the propyl substituent participates in close van der Waals contacts, and the ethoxy substituent occupies a pocket with mostly hydrophobic amino acid residues. The methylpiperazine group is exposed at the protein surface through the opening to the active site. Its interactions with the surrounding hydrophobic residues are not found in the equivalent region of PDE4-ligand complexes and presumably contribute to the selectivity of sildenafil for PDE5. Notably, sildenafil's sulfonyl group, a strong hydrogen-bond acceptor, is not involved in any hydrogen bonding.[47,49] Sildenafil and vardenafil differ in the heterocyclic ring system used to mimic the purine ring of cGMP and also differ in the substituent at the piperazine ring (sildenafil: methyl, vardenafil: ethyl; Figure 5). However, the higher biochemical potency of vardenafil over sildenafil has been largely attributed to the successful scaffold leap to the different heterocyclic core.[50]

To gain further insight into the SAR at the piperazine position and to investigate possible implications on the in vitro pharmacokinetic properties, the sulfoximine analogue **29** of vardenafil was prepared in an opportunistic approach. The synthesis of sulfoximine analogue **29** was accomplished in just two steps. Addition of sulfoximine building block **4** (see Scheme 1) to the commercial sulfonyl chloride **27**, followed by removal of the trifluorocarbonyl group at the sulfoximine nitrogen under basic conditions, yielded the desired sulfoximine **29** (Scheme 7).

Gratifyingly, sulfoximine analogue **29** proved to be a very potent PDE5 inhibitor. With an IC_{50} of 0.025 nM in the in vitro PDE5 enzyme assay,[51] compound **29** is basically equipotent with vardenafil (IC_{50} = 0.029 nM, Table 4).

The thermodynamic solubility of vardenafil in water at pH 6.5 is higher than that of analogue **29** (220 mg L^{-1} for vardenafil vs. 52 mg L^{-1} for **29**). Sulfoximine analogue **29** exhibited a significantly decreased log*D* value of 2.0 relative to 2.6 for vardenafil.

In vitro pharmacokinetic studies with vardenafil and sulfoximine **29** revealed a similar trend as in the other examples in this study in which an amine was exchanged for a sulfoximine group. Analogue **29** displayed improved in vitro stability in rat hepatocytes and human liver microsomes. However, in the Caco2 screening assay, vardenafil had a high permeability coefficient (P_{app} A→B) of 206 nm s^{-1} and efflux ratio of 0.87 where-

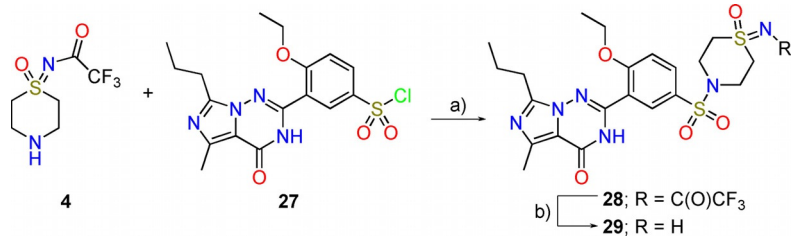

Scheme 7. Synthesis of vardenafil analogue **29**. *Reagents and conditions*: a) Et_3N (1 equiv), CH_2Cl_2, RT, 24 h; b) K_2CO_3, MeOH, RT, 90 min, 35% (2 steps).

Table 4. Comparison of the in vitro properties of vardenafil and sulfoximine analogue **29**.

Compd	IC_{50} [nM][a] PDE5	S_w pH 6.5 [mg L^{-1}][b]	log*D* pH 7.5[c]	CL_b [L h^{-1} kg^{-1}][d] rHep	hLMs	P_{app} A→B [nm s^{-1}][e]	ER[e]
vardenafil	0.029	220	2.6	3.0	1.1	206	0.87
29	0.025	52	2.0	2.1	0.43	0.71	288

[a] IC_{50} values determined in a PDE5 enzyme assay using [^{3}H]-cGMP as substrate, measured via a scintillation proximity assay technique.[51] [b] Thermodynamic solubility in water determined by an equilibrium shake flask method;[39] solid state of the test compounds was not characterized. [c] Determined by reversed-phase HPLC.[29] [d] Predicted hepatic metabolic clearance based on a high-throughput metabolic stability assay using 1) freshly harvested rat hepatocytes (rHep) and 2) pooled human liver microsomes (hLMs).[30] [e] P_{app} A→B (apical to basolateral) and efflux ratio (ER) data were generated in a bidirectionally performed Caco2 permeability assay in a 24-well format; ER was calculated as P_{app} B→A/P_{app} A→B.[30]

as sulfoximine analogue **29** had a very low permeability coefficient (P_{app} A→B) of <1 nm s^{-1} and a high efflux ratio of >200 (Table 4). It can be argued that the TPSA of sulfoximine analogue **29** is not within the Veber rule[52] and, additionally, that its molecular weight exceeds the rule of five (see Table 6). However, the extent of the difference in the in vitro permeability properties of vardenafil and its analogue **29** is still surprising.

Fulvestrant

Although selective estrogen receptor modulators, such as tamoxifen, or aromatase inhibitors, such as anastrozole, are the preferred endocrine treatment approach for most patients with HR+ breast cancer, many patients experience disease progression despite this therapy or the tumor becomes therapy-resistant.[53] Fulvestrant (Figure 6) is a steroid-based, selective estrogen receptor degrader (SERD) that both antagonizes and degrades ER-α and is active in patients experiencing disease progression on antihormonal agents. In contrast to some other antitumor agents, sustained exposure to fulvestrant via chronic administration is required for activity. Fulvestrant is a particularly lipophilic molecule, even relative to other steroidal compounds, with extremely low aqueous solubility, at an estimated 10 ng mL^{-1}.[54] Therefore, significant research has been conducted on the identification of suitable pharmaceutical formulations. Oral delivery has been explored using a range of formulations; however, the low level of bioavailability and presystemic metabolism mean that this is not an appropriate route of administration.[55] Hence, a long-acting, intramuscular (i.m.) formulation of fulvestrant was developed. Fulvestrant is highly metabolized across species, both in vitro and in vivo. After i.v. or i.m. delivery in humans, fulvestrant is converted at the 3- and 17-positions of the steroid nucleus to form ketone, sulfate, and glucuronide metabolites, and at the 9′-position to form the sulfone metabolite **30** (Figure 6).[56]

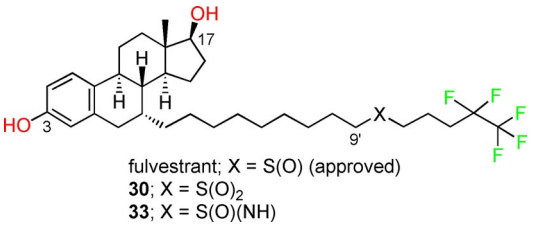

fulvestrant; X = S(O) (approved)
30; X = $S(O)_2$
33; X = S(O)(NH)

Figure 6. Structures of selective estrogen receptor modulator fulvestrant, sulfone metabolite **30**, and sulfoximine analogue **33**.

To investigate the impact of an exchange from sulfoxide to sulfoximine at the 9′-position on biological activity, physicochemistry, and in vitro metabolism, the sulfoximine analogue **33** was prepared. This target molecule would also provide an interesting opportunity to evaluate the feasibility of novel, safe imination procedures when applied to complex compounds. In our experience, the conversion of a sulfoxide into a sulfoximine can result in complex product mixtures in poor yields involving difficult purification procedures, or even that it fails completely, depending on the chemical nature of the starting material.[11]

The synthesis of analogue **33** was carried out from commercially available fulvestrant (Scheme 8). Various literature imination procedures[9a,g,57] were tested in an attempt to directly obtain the sulfoximine in one synthetic step. Unfortunately, these reactions resulted in insufficient conversions and complex product mixtures. We suspected that the unprotected hydroxy groups, especially the phenoxy group, were the root

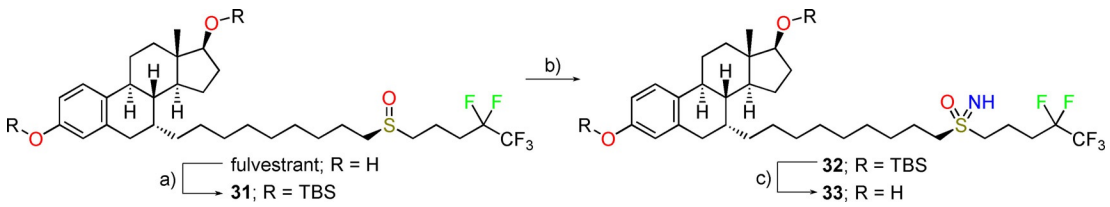

Scheme 8. Synthesis of fulvestrant analogue **33**. *Reagents and conditions*: a) TBSCl (4 equiv), imidazole (10 equiv), DMF, RT, 16 h, 95%; b) $H_2NCO_2NH_4$ (4 equiv), $PhI(OAc)_2$ (3 equiv), MeOH, RT, 2 h, 70%; c) TBAF (4.5 equiv), THF, 60 °C, 4 h, 68%.

cause of these problems and thus both hydroxy groups were protected with TBS (**31**) in one step prior to imination. Although known rhodium-catalyzed imination methods were employed successfully,[9a,g] the simplicity of the new noncatalytic procedure reported by Luisi, Bull, and co-workers,[57] using ammonium carbamate as the iminating agent, drew our attention. This method allowed preparation of the free sulfoximine **32** under mild conditions in a 70% yield (Scheme 8). Final deprotection of both hydroxy groups with TBAF afforded fulvestrant analogue **33**.

Fulvestrant and its sulfoximine analogue **33** both had very potent in vitro activities in a wild-type estrogen receptor 1 transactivation assay,[58] with an IC_{50} of 2.0 nM and of 1.8 nM, respectively. Furthermore, analogue **33** also exhibited very potent antiproliferative activity in vitro against human MCF7 cells stimulated with 17β-estradiol,[59] with an IC_{50} of 7.1 nM, very similar to the IC_{50} of 9.2 nM for fulvestrant (Table 5).

The switch from sulfoxide to sulfoximine at the 9′-position also resulted in a significant decrease in lipophilicity of analogue **33** with a log*D* value of 3.8 compared with 4.2 for fulvestrant. However, this did not translate into a measurable improvement in solubility. Fulvestrant and its analogue **33** both have aqueous solubility at pH 6.5 below the detection limit (< 0.1 mg L^{-1}), using the equilibrium shake flask method.[38]

In contrast to prior examples in this study, sulfoximine **33** did not display significantly improved in vitro stability over fulvestrant. Analogue **33** and fulvestrant both have low metabolic stability in rat hepatocytes with a high predicted CL_b of 3.5 L h^{-1} kg^{-1}. With human liver microsomes, sulfoximine **33** also revealed a very similar stability to fulvestrant (CL_b of 1.2 L h^{-1} kg^{-1} for fulvestrant vs. 1.1 L h^{-1} kg^{-1} for **33**, Table 5). Unfortunately, analogue **33** also did not show any improvement with regard to permeability properties. Both compounds, fulvestrant and its analogue **33**, exhibited no permeability in either direction (P_{app} A→B and P_{app} B→A) which may also be attributable to precipitation and extensive sticking to plastics during the incubation period (90 min).

Conclusions

After its late discovery, the sulfoximine group garnered only a very moderate interest in medicinal chemistry for many decades. In recent years, however, interest in sulfoximine chemistry has increased substantially, as evidenced by the development of new, safe methods for the preparation of sulfoximines, a significant increase in life science patent applications incorporating sulfoximine compounds, and the clinical evaluation of at least three novel sulfoximines, the kinase inhibitors roniciclib, BAY 1143572, and AZD 6738. Nevertheless, there remain gaps in the general understanding of this neglected functional group with respect to its medicinal chemistry relevant properties, which still need to be clarified. Very recently, Gnamm, Bolm, and co-workers evaluated the in vitro properties of a set of sulfoximines and concluded that sulfoximines do not have any "intrinsic flaw" and often exhibit favorable properties compared with other, more established functional groups in medicinal chemistry.[17]

Our study also aimed to shed further light on the medicinal chemistry relevant properties of sulfoximines. With this view in mind, we prepared a set of direct sulfoximine analogues of marketed drugs (imatinib, palbociclib, vardenafil, fulvestrant) and advanced clinical candidates (AT7519, ribociclib) to compare the in vitro properties of the matched molecular pairs.

This work could not be expected to deliver a general guideline for chemists in the life sciences as to when the introduction of a sulfoximine group should be considered. This is not only due to the limited number of analogues investigated, but also because our approach was based on an opportunistic, late-stage exchange of one functional group in compounds which had already been thoroughly optimized for the treatment of human diseases. Furthermore, it is known that the overall properties of a compound are determined by the "Gesamtkunstwerk" (complete work of art) and not solely by one functional group. Nevertheless, the results from this study contribute new pieces to the emerging picture of sulfoximines as pharmacophores and support previous findings that there seems to be no intrinsic flaw of this neglected functional group. For instance, the metabolic stability of sulfoximines was not identified as an issue in our study. The analogues of imatinib, palbociclib, ribociclib, and vardenafil all revealed a trend for improved metabolic stabilities in pharmacokinetic studies in vitro, and sulfoximine **15** was significantly more stable in rat hepatocytes and human liver microsomes than its matched pair AT7519. With respect to lipophilicity, very similar log*D* values were recorded for the amines imatinib, AT7519, palbociclib, and ribociclib, and their corresponding sulfoximine analogues (**8**, **15**, **23**, **26**). A more pronounced difference was noted for the analogues of the ethylpiperazine vardenafil and

Table 5. Comparison of the in vitro properties of fulvestrant and sulfoximine analogue **33**.

Compd	IC_{50} [nM]		S_w pH 6.5 [mg L^{-1}][c]	log*D* pH 7.5[d]	CL_b [L h^{-1} kg^{-1}][e]		P_{app} A→B [nm s^{-1}][f]	ER[f]
	ESR1 WT[a]	MCF7 E2 stim.[b]			rHep	hLMs		
fulvestrant	2.0	9.2	< 0.1	4.2	3.5	1.2	0	0
33	1.8	7.1	< 0.1	3.8	3.5	1.1	0	0

[a] IC_{50} values determined in a wild-type estrogen receptor 1 (ESR1) transactivation assay.[58] [b] IC_{50} values determined in an in vitro proliferation assay using human MCF7 cells stimulated with 17β-estradiol (E2).[59] [c] Thermodynamic solubility in water determined by an equilibrium shake flask method;[39] solid state of the test compounds was not characterized. [d] Determined by reversed-phase HPLC.[29] [e] Predicted hepatic metabolic clearance based on a high-throughput metabolic stability assay using 1) freshly harvested rat hepatocytes (rHep) and 2) pooled human liver microsomes (hLMs).[30] [f] P_{app} A→B (apical to basolateral) and efflux ratio (ER) data were generated in a bidirectionally performed Caco2 permeability assay in a 24-well format; ER was calculated as P_{app} B→A/P_{app} A→B.[30]

the sulfoxide fulvestrant. In both cases, the log*D* value of the sulfoximine analogue (**29**, **33**) was decreased. In comparison with the amines in this study, the corresponding sulfoximine analogues do not show superior aqueous solubility at pH 6.5. The matched pair analogues of imatinib and palbociclib have similar solubility, whereas the analogues of AT7519, ribociclib, and vardenafil have significantly lower solubility at pH 6.5. The extremely low aqueous solubility of fulvestrant was confirmed in our assay; however, the sulfoximine analogue **33** with its lower log*D* value does not exhibit an improved aqueous solubility. It should be noted, however, that in this study the solid state of the test compounds, which can influence the solubility properties significantly, was not assessed (e.g., by X-ray powder diffraction).

In contrast to our previous findings with roniciclib[13b,14] and BAY 1143572,[15b,c] the current results indicate that permeability and efflux can be an issue when a sulfoximine group is introduced. With the exception of compound **15**, all analogues in this study displayed decreased permeability and increased efflux. Most striking is the significant loss of permeability and increased efflux that was recorded with the analogue **29** of vardenafil. Unfortunately, the permeability properties of fulvestrant and its analogue **33** could not be properly assessed due to the very low solubility and high lipophilicity of these compounds. As noted, this investigation used late-stage exchange of a functional group in optimized compounds, and some of the resulting sulfoximines are borderline with respect to accepted drug-like score rules (Table 6); however, our results indicate that the permeability properties of sulfoximines should be evaluated early. Use of the corresponding *N*-methyl sulfoximines may improve the permeability properties.[17]

With regard to in vitro potency, our results are very promising. The analogues of the kinase inhibitors imatinib, AT7519, and palbociclib all have sub-micromolar activities in the relevant biochemical assays. These compounds also exhibit modulated kinase selectivity profiles, which is surprising because the sulfoximine groups are expected to be directed toward the exit of the kinase binding pockets. The biochemical activity of these compounds also translated into good cellular activities with promising antiproliferative effects of sulfoximines **15** and **23** in vitro. Moreover, both sulfoximines **29** and **33** displayed at least equipotent activity as vardenafil and fulvestrant, respectively, in the corresponding biochemical assays. Sulfoximine **33** also had low-nanomolar activity in the cellular antiproliferation assay using MCF7 cells, being at least as potent as fulvestrant.

Overall, these new results further support the earlier recommendation that the sulfoximine moiety be added to the medicinal chemist's toolbox, thus broadening the chemical repertoire in small-molecule drug discovery to tackle biological targets in an even more multifaceted manner.[6] Accordingly, further innovations in sulfoximine synthetic methodology, along with a significant increase in commercial sulfoximine building blocks, would help to accelerate the field of sulfoximines as pharmacophores in the life sciences.

Table 6. Molecular weight (MW), topological polar surface area (TPSA), and number of hydrogen-bond donors (HBD) and acceptors (HBA) of the test compounds in this study.

Compd	MW [Da]	TPSA [Å^2]	HBD[a]	HBA[b]
imatinib	493.60	86.28	2	7
8	527.64	123.96	3	8
AT7519	382.24	98.91	4	4
15	430.31	127.89	4	5
palbociclib	447.53	103.35	2	8
23	495.60	132.24	2	9
ribociclib	434.54	91.21	2	7
26	482.60	120.10	2	8
vardenafil	488.60	109.12	1	7
29	508.61	146.80	2	8
fulvestrant	606.77	57.53	2	3
33	621.79	81.38	3	4

[a] HBD: number of heteroatoms (O, N, P, S) with one or more attached hydrogen atoms. [b] HBA: number of heteroatoms (O, N, P, S) with one or more lone pairs, excluding atoms with formal positive charges, amide and pyrrole-type nitrogen atoms, and aromatic oxygen and sulfur atoms in heterocyclic rings.

Experimental Section

Commercially available reagents and anhydrous solvents were used without further purification. All air- and moisture-sensitive reactions were carried out in oven-dried (at 120 °C) glassware under an inert atmosphere of argon. Reactions were monitored by TLC and UPLC analysis with a Waters Acquity UPLC MS Single Quad system; column: Acquity UPLC BEH C_{18} 1.7 μm, 50×2.1 mm; eluent A: H_2O + 0.2 vol% aq. NH_3 (32%), eluent B: MeCN; gradient: 0–1.6 min 1–99% B, 1.6–2.0 min 99% B; flow: 0.8 mL min^{-1}; temperature: 60 °C; DAD scan: 210–400 nm. Flash chromatography was carried out using a Biotage® Isolera™ One system with 200–400 nm variable detector, using Biotage® SNAP KP-Sil or KP-NH cartridges. Preparative HPLC was carried out with a Waters AutoPurification MS Single Quad system; column: Waters XBridge C_{18} 5 μm, 100×30 mm; eluent A: H_2O + 0.2 vol% aq. NH_3 (32%), eluent B: MeCN; gradient: 0–5.5 min 5–100% B; flow: 70 mL min^{-1}; temperature: 25 °C; DAD scan: 210–400 nm. Analytical TLC was carried out on aluminum-backed plates coated with Merck Kieselgel 60 F_{254}, with visualization under UV light at 254 nm. All NMR spectra were recorded on Bruker Avance III HD spectrometers. ^{1}H NMR spectra were obtained at 300, 400, 500, or 600 MHz and referenced to the residual solvent signal (7.26 ppm for $CDCl_3$). ^{13}C NMR spectra were obtained at 101 or 151 MHz and also referenced to the residual solvent signal (77.16 ppm for $CDCl_3$). All spectra were obtained at ambient temperature (22 ± 1 °C). ^{1}H NMR data are reported as follows: chemical shift (δ) in ppm, multiplicity (s = singlet, d = doublet, t = triplet, q = quartet, quin = quintuplet, sxt = sextuplet, br = broad, m = multiplet), coupling constant(s) (Hz), and integration. Mass spectra were recorded on LC–MS instruments: 1) Waters Acquity UPLC MS Single Quad system; column: Kinetex 2.6 μm, 50×2.1 mm, or 2) Agilent 1290 UPLC MS 6230 TOF system; column: BEH C_{18} 1.7 μm, 50×2.1 mm; eluent A: H_2O + 0.05% formic acid (99%), eluent B: MeCN + 0.05% formic acid (99%). Fragment ions are reported as *m/z* values with relative intensities (%) in parentheses. High-resolution mass spectra were recorded on a Xevo® G2-XS QTof (Waters) instrument. Melting points were determined with a Büchi B-540 melting point apparatus.

Benzyl thiomorpholine-4-carboxylate (1): A round-bottom flask charged with thiomorpholine (100 g, 969 mmol) and aq. NaOH

(1.0 M, 580 mL, 580 mmol) was cooled to 0 °C. Benzyl chloroformate (83 mL, 589 mmol) was added dropwise and the reaction mixture was stirred for 1 h at 0 °C and then for 3 h at RT. Then, the mixture was neutralized with aq. HCl (1.0 M) and extracted with EtOAc (2×). The combined organic layer was washed with sat. aq. NaCl, dried (Na_2SO_4), filtered, and concentrated to afford **1** as a brown oil (138 g, 581 mmol, 98%): ^{1}H NMR (300 MHz, $CDCl_3$): δ = 7.27–7.42 (m, 5H), 5.14 (s, 2H), 3.71–3.82 (m, 4H), 2.50–2.68 ppm (m, 4H).

Benzyl thiomorpholine-4-carboxylate 1-oxide (2): To a stirred solution of sulfide **1** (93 g, 392 mmol) in MeCN (928 mL) was added $FeCl_3$ (1.8 g, 11.2 mmol) and the reaction mixture was stirred for 10 min at RT. Then, H_5IO_6 (95.5 g, 419 mmol) was added in three portions. The reaction was slightly exothermic and a water bath at ≈10 °C was used to control the temperature. The starting material was consumed after 3 h. Then, the reaction mixture was added to sat. aq. $Na_2S_2O_3$ (3 L) and stirred for 72 h at RT. The organic phase was separated and the aqueous layer was extracted with THF (2×). The combined organic layer was washed with sat. aq. NaCl, dried (Na_2SO_4), filtered, and concentrated to give **2** (107 g, crude): ^{1}H NMR (400 MHz, $CDCl_3$): δ = 7.28–7.41 (m, 5H), 5.14 (s, 2H), 3.80–4.19 (m, 4H), 2.59–2.92 ppm (m, 4H).

Benzyl 1-oxo-1-[(2,2,2-trifluoroacetyl)imino]-1λ^6-thiomorpholine-4-carboxylate (3): A mixture of crude sulfoxide **2** (47 g, 185 mmol), 2,2,2-trifluoroacetamide (42 g, 370 mmol), MgO (30 g, 739 mmol), $Rh_2(OAc)_4$ (1.9 g, 4.3 mmol), and $PhI(OAc)_2$ (89 g, 277 mmol) in CH_2Cl_2 (1.4 L) was stirred under argon at RT for 20 h. The suspension was filtered and the filtrate was concentrated. The crude was recrystallized from diisopropyl ether to afford **3** as a white solid (30.2 g, 83 mmol, 45%): ^{1}H NMR (300 MHz, $CDCl_3$): δ = 7.30–7.43 (m, 5H), 5.18 (s, 2H), 4.16–4.36 (m, 2H), 3.82 (ddd, J = 14.8, 8.7, 2.8 Hz, 2H), 3.65–3.76 (m, 2H), 3.25–3.43 ppm (m, 2H).

2,2,2-Trifluoro-*N*-(1-oxo-1λ^6-thiomorpholin-1-ylidene)acetamide (4): Pd/C (10 wt% Pd, 160 mg, 0.15 mmol) was added to a solution of sulfoximine **3** (547 mg, 1.5 mmol) in MeOH (15 mL). The reaction mixture was stirred vigorously at RT under an H_2 atmosphere (1 atm) for 5 h. The resulting suspension was filtered through a Hirsch filter and the filtrate was concentrated to give **4** as a white solid (342 mg, crude): ^{1}H NMR (400 MHz, $CDCl_3$): δ = 3.70–3.78 (m, 2H), 3.49 (s, 1H), 3.40–3.48 (m, 2H), 3.22–3.36 ppm (m, 4H).

4-(Chloromethyl)-*N*-(4-methyl-3-{[4-(pyridin-3-yl)pyrimidin-2-yl]amino}phenyl)benzamide (6): A suspension containing commercial **5** (700 mg, 2.5 mmol) and K_2CO_3 (733 mg, 5.3 mmol) in THF (10 mL) was cooled to 0 °C. A solution of 4-(chloromethyl)benzoyl chloride (525 mg, 2.8 mmol) in THF (3 mL) was added. The reaction mixture was stirred at 0 °C for 2 h and then at RT for 2 h. H_2O (20 mL) was slowly added and the mixture was stirred at RT for 30 min. The mixture was filtered and the residue was washed with H_2O and dried under reduced pressure to give **6** as a white solid (1.08 g, 2.5 mmol, 99%): ^{1}H NMR (400 MHz, [D$_6$]DMSO): δ = 10.25 (s, 1H), 9.28 (d, J = 1.7 Hz, 1H), 8.99 (s, 1H), 8.68 (dd, J = 4.7, 1.5 Hz, 1H), 8.51 (d, J = 5.1 Hz, 1H), 8.48 (dt, J = 8.2, 2.0 Hz, 1H), 8.09 (d, J = 1.9 Hz, 1H), 7.97 (s, 1H), 7.95 (s, 1H), 7.60 (s, 1H), 7.57 (s, 1H), 7.46–7.55 (m, 2H), 7.43 (d, J = 5.1 Hz, 1H), 7.21 (d, J = 8.5 Hz, 1H), 4.84 (s, 2H), 2.23 ppm (s, 3H).

4-[(1-Imino-1-oxo-1λ^6-thiomorpholin-4-yl)methyl]-*N*-(4-methyl-3-{[4-(pyridin-3-yl)pyrimidin-2-yl]amino}phenyl)benzamide (8): A mixture of **6** (124 mg, 0.29 mmol), crude sulfoximine **4** (100 mg, 0.43 mmol), and Et_3N (81 μL, 0.58 mmol) in DMF (1 mL) was held at reflux for 24 h. After cooling, the mixture was concentrated and the residue was dissolved in MeOH (1 mL). K_2CO_3 (80 mg, 0.58 mmol) was added and the mixture was stirred at RT for 1 h before it was diluted with sat. aq. NaCl and extracted with EtOAc (2×). The combined organic layer was filtered over a Whatman filter and concentrated. The residue was purified by preparative HPLC to give **8** (8 mg, 0.01 mmol, 5%): ^{1}H NMR (600 MHz, $CDCl_3$): δ = 9.26 (s, 1H), 8.70 (d, J = 4.1 Hz, 1H), 8.59 (s, 1H), 8.51 (d, J = 4.9 Hz, 1H), 8.49 (d, J = 7.9 Hz, 1H), 7.96 (s, 1H), 7.86 (d, J = 7.9 Hz, 2H), 7.40–7.46 (m, 3H), 7.29–7.34 (m, 1H), 7.21 (d, J = 8.3 Hz, 1H), 7.18 (d, J = 5.3 Hz, 1H), 7.07 (s, 1H), 3.70 (s, 2H), 3.04–3.17 (m, 4H), 2.90–3.02 (m, 4H), 2.61 (s, 1H), 2.35 ppm (s, 3H); ^{13}C NMR (151 MHz, $CDCl_3$): δ = 165.3, 162.9, 160.7, 159.2, 151.6, 148.7, 141.6, 137.9, 136.6, 135.1, 134.7, 132.8, 131.0, 129.2, 127.5, 124.4, 123.9, 115.4, 113.2, 108.6, 61.3, 53.7, 50.9, 17.9 ppm; MS (ES$^-$) *m/z* (%): 527 (33) [M^+], 526 (100), 572 (27), 528 (11).

Benzyl tetrahydro-2*H*-thiopyran-4-ylcarbamate (9): A round-bottom flask charged with tetrahydro-2*H*-thiopyran-4-amine (50.0 g, 427 mmol) and aq. NaOH (1.0 M, 500 mL, 500 mmol) was cooled to 5 °C. Benzyl chloroformate (60 mL, 427 mmol) was added dropwise and the reaction mixture was stirred at RT for 1 h. Then, the mixture was extracted with CH_2Cl_2 (3×). The combined organic layer was washed with sat. aq. NaCl, dried (Na_2SO_4), filtered, and concentrated. The crude was suspended in hexanes and filtered in a Büchner funnel to afford **9** as a white solid (62.5 g, 249 mmol, 58%): ^{1}H NMR (400 MHz, $CDCl_3$): δ = 7.29–7.43 (m, 5H), 5.09 (br s, 2H), 4.70 (br s, 1H), 3.44–3.63 (m, 1H), 2.59–2.87 (m, 4H), 2.24 (br d, J = 12.6 Hz, 2H), 1.48–1.62 ppm (m, 2H).

Benzyl 1-oxidotetrahydro-2*H*-thiopyran-4-ylcarbamate (10): To a stirred suspension of sulfide **9** (62.5 g, 249 mmol) in MeCN (600 mL) was added $FeCl_3$ (1.13 g, 7 mmol), followed by H_5IO_6 (60 g, 264 mmol) in two portions. The reaction was slightly exothermic and a water bath at ≈10 °C was used to control the temperature. The mixture was stirred at RT for 3 h before it was added to sat. aq. $Na_2S_2O_3$ and extracted with EtOAc (3×). The combined organic layer was dried (Na_2SO_4), filtered, and concentrated to give **10** as a white solid (66.4 g, 248 mmol, quant.): ^{1}H NMR (300 MHz, $CDCl_3$): δ = 7.30–7.42 (m, 5H), 5.10 (s, 2H), 4.77–4.97 (m, 1H), 3.57–3.88 (m, 1H), 3.01–3.14 (m, 2H), 2.36–2.61 (m, 2H), 2.09–2.34 (m, 2H), 1.91–2.07 (m, 1H), 1.77 ppm (br s, 1H).

Benzyl *N*-{1-oxo-1-[(2,2,2-trifluoroacetyl)imino]-1λ^6-thian-4-yl}carbamate (11): A mixture of sulfoxide **10** (66.4 g, 248 mmol), 2,2,2-trifluoroacetamide (56.1 g, 497 mmol), MgO (40.0 g, 993 mmol), $Rh_2(OAc)_4$ (5.5 g, 12.4 mmol), and $PhI(OAc)_2$ (120.0 g, 373 mmol) in CH_2Cl_2 (1.6 L) was stirred under argon at RT for 72 h. The suspension was filtered through Celite with suction and the filtrate was concentrated. The residue was purified by flash chromatography (CH_2Cl_2/*i*PrOH, 95:5) to afford **11** as a white solid (33.0 g, 87.2 mmol, 35%): ^{1}H NMR (400 MHz, [D$_6$]DMSO): δ = 7.51 (br d, J = 7.8 Hz, 1H), 7.27–7.42 (m, 5H), 5.02 (s, 2H), 3.67–3.81 (m, 1H), 3.14–3.28 (m, 2H), 2.99–3.12 (m, 2H), 2.00–2.16 (m, 2H), 1.80–1.97 ppm (m, 2H).

***N*-(4-Amino-1-oxo-1λ^6-thian-1-ylidene)-2,2,2-trifluoroacetamide(12)**: Pd/C (10 wt% Pd, 78 mg, 0.07 mmol) was added to a solution of sulfoximine **11** (400 mg, 1.06 mmol) in MeOH (38 mL) and THF (19 mL), and the mixture was stirred for 5 h at RT under an H_2 atmosphere (1 atm). The mixture was filtered and the filtrate was concentrated to give crude amine **12** (254 mg) that was used without further purification.

4-(2,6-Dichlorobenzamido)-*N*-{1-oxo-1-[(2,2,2-trifluoroacetyl)imino]-1λ^6-thian-4-yl}-1*H*-pyrazole-3-carboxamide (14) and 4-(2,6-Dichlorobenzamido)-*N*-(1-imino-1-oxo-1λ^6-thian-4-yl)-1*H*-pyra-

zole-3-carboxamide (15): A mixture of commercial acid **13** (268 mg, 0.89 mmol), crude amine **12** (240 mg), *N*-(3-dimethylaminopropyl)-*N*′-ethylcarbodiimide (166 mg, 1.07 mmol), and 1-hydroxybenzotriazole (145 mg, 1.07 mmol) in DMF (3 mL) was stirred at RT for 42 h. The reaction mixture was diluted with EtOAc, washed with sat. aq. $NaHCO_3$, filtered through a Whatman filter, and concentrated. The residue was purified by preparative HPLC (eluents: A: H_2O + 0.1% HCO_2H, B: MeCN) to afford **14** as a white solid (63 mg, 0.11 mmol, 12%) and **15** as a white solid (85 mg, 0.19 mmol, 20%).

14: ^{1}H NMR (500 MHz, [D_6]DMSO): δ = 13.55 (br s, 1H), 9.93 (br s, 1H), 9.42 (br s, 1H), 8.15–8.38 (m, 1H), 7.53–7.57 (m, 2H), 7.47–7.52 (m, 1H), 4.10–4.23 (m, 1H), 3.82 (m, 2H), 3.63–3.73 (m, 2H), 1.91–2.25 ppm (m, 4H); MS (ES$^+$) *m/z* (%): 526 (72) [M^+ + H], 524 (100), 525 (16), 528 (10).

15: ^{1}H NMR (500 MHz, [D_6]DMSO): δ = 13.40 (br s, 1H), 10.14 (s, 1H), 8.55 (br s, 1H), 8.33 (br s, 1H), 7.56–7.60 (m, 2H), 7.50–7.54 (m, 1H), 4.01–4.13 (m, 1H), 3.46 (s, 1H), 3.10–3.19 (m, 2H), 3.01 (m, 2H), 2.06–2.20 (m, 2H), 1.97 ppm (m, 2H); MS (ES$^+$) *m/z* (%): 430 (100) [M^+ + H], 432 (69), 431 (21), 434 (16), 433 (14).

4-(6-Nitropyridin-3-yl)thiomorpholine (16): A mixture of 5-bromo-2-nitropyridine (1.02 g, 5.0 mmol) and thiomorpholine (0.77 g, 7.5 mmol) was heated for 1 h at 120 °C. After cooling, the residue was suspended in DMSO (1 mL) and H_2O (10 mL) using a sonication bath. The yellow suspension was filtered through a Hirsch funnel, and the solid was washed successively with H_2O, EtOH, and Et_2O, and dried at 40 °C under vacuum, affording crude **16** (1.12 g) that was used without further purification: ^{1}H NMR (400 MHz, [D_6]DMSO): δ = 8.25 (d, *J* = 3.3 Hz, 1H), 8.15 (d, *J* = 9.4 Hz, 1H), 7.48 (dd, *J* = 9.4, 3.0 Hz, 1H), 3.81–4.00 (m, 4H), 2.62–2.75 ppm (m, 4H).

4-(6-Nitropyridin-3-yl)thiomorpholine 1-oxide (17): Sulfide **16** (1.12 g, 5.0 mmol) was suspended in aq. H_2O_2 (30%, 5.1 mL, 49.7 mmol) and the mixture was stirred at RT for 4 h. Then, it was diluted with H_2O and filtered. The solid was washed successively with H_2O/DMSO (4:1), H_2O, EtOH, and Et_2O, and finally dried at 40 °C under vacuum for 6 h to give **17** as a yellow solid (743 mg, 3.1 mmol, 62%): ^{1}H NMR (400 MHz, [D_6]DMSO): δ = 8.35 (d, *J* = 3.3 Hz, 1H), 8.19 (d, *J* = 9.4 Hz, 1H), 7.60 (dd, *J* = 9.3, 3.2 Hz, 1H), 3.94–4.11 (m, 4H), 2.89–3.03 (m, 2H), 2.69–2.78 ppm (m, 2H).

***tert*-Butyl *N*-[4-(6-nitropyridin-3-yl)-1-oxo-1λ^6-thiomorpholin-1-ylidene]carbamate (18)**: To a stirred suspension of sulfoxide **17** (580 mg, 2.4 mmol), *tert*-butyl carbamate (426 mg, 3.6 mmol), $Rh_2(OAc)_4$ (27 mg, 0.06 mmol), and MgO (390 mg, 9.7 mmol) in 1,2-dichloroethane (24 mL) was added $PhI(OAc)_2$ (1171 mg, 3.6 mmol) at RT. The resulting mixture was stirred at 40 °C for 5 h. The reaction mixture was diluted with EtOAc, filtered through a pad of diatomaceous earth, and concentrated. The residue was purified by flash chromatography (hexane/EtOAc, 1:2) to afford **18** as a yellow solid (740 mg, 2.0 mmol, 83%): R_f = 0.21 (hexane/EtOAc, 1:2); mp: 196–198 °C; ^{1}H NMR (400 MHz, $CDCl_3$): δ = 8.21 (d, *J* = 3.0 Hz, 1H), 8.19 (d, *J* = 9.1 Hz, 1H), 7.34 (dd, *J* = 9.1, 3.0 Hz, 1H), 4.11–4.20 (m, 2H), 3.99 (ddd, *J* = 15.1, 8.5, 2.3 Hz, 2H), 3.69–3.79 (m, 2H), 3.35–3.48 (m, 2H), 1.47 ppm (s, 9H); ^{13}C NMR (101 MHz, $CDCl_3$): δ = 158.2, 149.0, 147.4, 134.7, 122.5, 120.0, 81.4, 49.4, 45.7, 28.2 ppm; MS (ES$^+$) *m/z* (%): 401 (100) [M^+ + HCO_2H − H], 402 (19), 355 (5); HRMS (ES$^+$) *m/z* [M^+ − $C_5H_8O_2$ + H] calcd for $C_9H_{13}N_4O_3S$: 257.0703, found: 257.0708.

***tert*-Butyl *N*-[4-(6-aminopyridin-3-yl)-1-oxo-1λ^6-thiomorpholin-1-ylidene]carbamate (19)**: Pd/C (10 wt% Pd, 159 mg, 0.15 mmol) was added to a solution of **18** (530 mg, 1.49 mmol) in EtOH (50 mL). The resulting suspension was vigorously stirred at RT under an H_2 atmosphere (1 atm) for 2 h. The reaction mixture was filtered through a pad of diatomaceous earth and concentrated. The residue was purified by flash chromatography (CH_2Cl_2/MeOH, 95:5) to afford **19** as a yellow solid (329 mg, 1.01 mmol, 68%): R_f = 0.18 (CH_2Cl_2/MeOH, 95:5); mp: 121–123 °C; ^{1}H NMR (400 MHz, $CDCl_3$): δ = 7.82 (d, *J* = 2.8 Hz, 1H), 7.18 (dd, *J* = 8.7, 2.9 Hz, 1H), 6.49 (d, *J* = 8.9 Hz, 1H), 4.32 (br s, 2H), 3.65–3.73 (m, 2H), 3.49–3.64 (m, 4H), 3.38–3.47 (m, 2H), 1.49 ppm (s, 9H); ^{13}C NMR (101 MHz, $CDCl_3$): δ = 158.6, 154.6, 139.5, 138.4, 130.5, 109.3, 81.0, 50.2, 49.5, 28.3 ppm; MS (ES$^+$) *m/z* (%): 271 (100) [M^+ − C_4H_8 + H], 272 (14), 227 (8).

***tert*-Butyl *N*-{4-[6-({6-bromo-8-cyclopentyl-5-methyl-7-oxo-7H,8*H*-pyrido[2,3-*d*]pyrimidin-2-yl}amino)pyridin-3-yl]-1-oxo-1λ^6-thiomorpholin-1-ylidene}carbamate (21)**: *i*PrMgCl (2 M in THF, 0.27 mL, 0.53 mmol) was added dropwise to a suspension of **19** (158 mg, 0.48 mmol) in anhydrous THF (2 mL) at 0 °C. A suspension of commercial chloride **20** (166 mg, 0.48 mmol) in THF (1 mL) was added dropwise to the mixture at 0 °C, which was then stirred at RT for 18 h. Additional *i*PrMgCl (2 M in THF, 0.24 mL, 0.48 mmol) was added and the mixture was stirred at RT for 1 h, before additional *i*PrMgCl (2 M in THF, 0.24 mL, 0.48 mmol) was added, and the mixture was finally stirred for 2 h. The reaction mixture was quenched with aq. HCl (0.5 M), giving a yellow precipitate that was washed in a Hirsch filter with H_2O, EtOH, and Et_2O. The residue was purified by preparative HPLC (MeCN/H_2O, gradient: 40–80% MeCN, + 0.1% HCO_2H) affording **21** as a yellow solid (45 mg, 0.07 mmol, 15%): R_f = 0.32 (CH_2Cl_2/MeOH, 95:5); mp: 195–199 °C; ^{1}H NMR (400 MHz, $CDCl_3$): δ = 8.82 (s, 1H), 8.26 (d, *J* = 9.1 Hz, 1H), 8.24 (br s, 1H), 8.09 (d, *J* = 2.8 Hz, 1H), 7.37 (dd, *J* = 9.0, 2.9 Hz, 1H), 5.98 (quin, *J* = 8.7 Hz, 1H), 3.79–3.91 (m, 2H), 3.68–3.78 (m, 4H), 3.40–3.50 (m, 2H), 2.62 (s, 3H), 2.26–2.37 (m, 2H), 2.06–2.18 (m, 2H), 1.84–1.95 (m, 2H), 1.59–1.76 (m, 2H), 1.50 ppm (s, 9H); MS (ES$^+$) *m/z* (%): 634 (100) [M^+(^{81}Br) + H], 632 (95), 635 (32), 633 (30); HRMS (ES$^+$) *m/z* [M^+ + H] calcd for $C_{27}H_{35}BrN_7O_4S$: 632.1655, found: 632.1656.

4-[6-({6-Acetyl-8-cyclopentyl-5-methyl-7-oxo-7H,8*H*-pyrido[2,3-*d*]pyrimidin-2-yl}amino)pyridin-3-yl]-1-imino-1λ^6-thiomorpholin-1-one (23): A stirred suspension of **21** (30.0 mg, 0.047 mmol), tributyl(1-ethoxyvinyl)tin (24 μL, 0.071 mmol), and $PdCl_2(PPh_3)_2$ (2.7 mg, 0.004 mmol) in anhydrous dioxane (0.5 mL) was heated at 100 °C under argon for 7 h. After cooling, 2 drops of aq. HCl (2 M) were added and the mixture was stirred at RT for 2 h. The mixture was diluted with CH_2Cl_2, dried (Na_2SO_4), filtered, and concentrated. The residue was dissolved in CH_2Cl_2 (3 mL) and trifluoroacetic acid (24 μL, 0.33 mmol) was added. The reaction mixture was stirred at RT for 1 h before sat. aq. $NaHCO_3$ was added. The mixture was extracted with CH_2Cl_2 (2×) and the combined organic layer was dried (Na_2SO_4), filtered, and concentrated. The residue was purified by chromatography (CH_2Cl_2/MeOH, 95:5) to give **23** as an orange solid (16 mg, 0.030 mmol, 64%): R_f = 0.15 (CH_2Cl_2/MeOH, 95:5); mp: 134–137 °C; ^{1}H NMR (400 MHz, $CDCl_3$): δ = 8.81 (s, 1H), 8.24 (d, *J* = 9.0 Hz, 1H), 8.07 (d, *J* = 2.6 Hz, 1H), 8.06 (br s, 1H), 7.36 (dd, *J* = 9.0, 3.0 Hz, 1H), 5.87 (quin, *J* = 8.8 Hz, 1H), 3.73–3.83 (m, 4H), 3.17–3.27 (m, 4H), 2.62 (br s, 1H), 2.55 (s, 3H), 2.38 (s, 3H), 2.29–2.40 (m, 2H), 2.03–2.12 (m, 2H), 1.84–1.93 (m, 2H), 1.67–1.74 ppm (m, 2H); ^{13}C NMR (101 MHz, $CDCl_3$): δ = 202.8, 161.5, 158.0, 157.3, 155.6, 146.2, 141.8, 141.1, 137.9, 131.2, 127.3, 113.8, 108.2, 54.1, 52.9, 48.8, 31.7, 28.3, 26.0, 14.2, 13.8 ppm; MS (ES$^+$) *m/z* (%): 496 (44) [M^+ + H], 249 (100), 497 (13); HRMS (ES$^+$) *m/z* [M^+ + H] calcd for $C_{24}H_{30}N_7O_3S$: 496.2131, found: 496.2130.

***tert*-Butyl *N*-[4-(6-{[7-cyclopentyl-6-(dimethylcarbamoyl)-7*H*-pyrrolo[2,3-*d*]pyrimidin-2-yl]amino}pyridin-3-yl)-1-oxo-1λ^6-thiomorpholin-1-ylidene]carbamate (25)**: A mixture of **19** (52 mg, 0.16 mmol), commercial chloride **24** (47 mg, 0.16 mmol), $Pd(OAc)_2$ (1.8 mg, 0.008 mmol), *rac*-BINAP (5.0 mg, 0.008 mmol), and Cs_2CO_3 (75 mg, 0.23 mmol) in anhydrous dioxane (1.3 mL) was stirred under argon in a sealed tube at 110 °C for 6 h. After cooling, H_2O (1 mL) was added and the mixture was extracted with EtOAc (2×). The combined organic layer was dried (Na_2SO_4), filtered, and concentrated. The residue was purified by chromatography (CH_2Cl_2/MeOH, 9:1) to give **25** as a yellow oil (66 mg, 0.11 mmol, 71%): R_f = 0.37 (CH_2Cl_2/MeOH, 95:5); ^{1}H NMR (400 MHz, $CDCl_3$): δ = 8.72 (s, 1H), 8.43 (d, J = 9.1 Hz, 1H), 8.07 (s, 1H), 8.06 (s, 1H), 7.35 (dd, J = 9.1, 3.0 Hz, 1H), 6.45 (s, 1H), 4.80 (quin, J = 8.9 Hz, 1H), 3.61–3.84 (m, 6H), 3.40–3.53 (m, 2H), 3.16 (s, 6H), 2.48–2.65 (m, 2H), 1.95–2.16 (m, 4H), 1.66–1.80 (m, 2H), 1.51 ppm (s, 9H).

7-Cyclopentyl-2-{[5-(1-imino-1-oxo-1λ^6-thiomorpholin-4-yl)pyridin-2-yl]amino}-*N*,*N*-dimethyl-7*H*-pyrrolo[2,3-*d*]pyrimidine-6-carboxamide (26): Trifluoroacetic acid (69 μL, 0.9 mmol) was added dropwise to a solution of **25** (75 mg, 0.13 mmol) in CH_2Cl_2 (0.3 mL) and the reaction mixture was stirred at RT for 5 h. Sat. aq. $NaHCO_3$ was added and the mixture was extracted with CH_2Cl_2 (2×). The combined organic layer was dried (Na_2SO_4), filtered, and concentrated. The residue was purified by chromatography (CH_2Cl_2/MeOH, 95:5) to give **26** as a white solid (42 mg, 0.09 mmol, 67%): R_f = 0.16 (CH_2Cl_2/MeOH, 95:5); mp: 238–241 °C; ^{1}H NMR (400 MHz, [D$_6$]DMSO): δ = 9.53 (s, 1H), 8.79 (s, 1H), 8.18 (d, J = 9.1 Hz, 1H), 8.11 (d, J = 3.0 Hz, 1H), 7.53 (dd, J = 9.3, 3.2 Hz, 1H), 6.60 (s, 1H), 4.74 (quin, J = 8.8 Hz, 1H), 3.71–3.84 (m, 3H), 3.54–3.64 (m, 2H), 2.98–3.12 (m, 10H), 2.43 (br dd, J = 11.5, 9.3 Hz, 2H), 1.89–2.05 (m, 4H), 1.55–1.73 ppm (m, 2H); ^{13}C NMR (101 MHz, [D$_6$]DMSO): δ = 162.9, 154.7, 152.2, 151.2, 146.4, 139.7, 136.3, 131.9, 126.0, 112.8, 111.9, 100.7, 57.0, 51.7, 47.8, 38.9, 34.7, 29.8, 24.3 ppm; MS (ES$^+$) *m*/*z* (%): 483 (25) [M^+ + H], 242 (100), 243 (28); HRMS (ES$^+$) *m*/*z* [M^+ + H] calcd for $C_{23}H_{31}N_8O_2S$: 483.2291, found: 483.2289.

4-(4-Ethoxy-3-{5-methyl-4-oxo-7-propyl-3H,4*H*-imidazo[4,3-*f*][1,2,4]triazin-2-yl}benzenesulfonyl)-1-imino-1λ^6-thiomorpholin-1-one (29): A solution of commercial sulfonyl chloride **27** (140 mg, 0.34 mmol), amine **4** (83 mg, 0.36 mmol), and Et_3N (50 μL, 0.36 mmol) in CH_2Cl_2 (3 mL) was stirred at RT for 24 h. The reaction mixture was diluted with sat. aq. NaCl and extracted with CH_2Cl_2 (2×). The combined organic layer was filtered through a Whatman filter and concentrated. The residue was dissolved in MeOH (5 mL) and solid K_2CO_3 (83 mg, 0.60 mmol) was added. The resulting suspension was stirred at RT for 90 min before it was diluted with sat. aq. NaCl and extracted with CH_2Cl_2 (2×). The combined organic layer was filtered through a Whatman filter and concentrated. The residue was purified by preparative HPLC (eluents: A: H_2O + 0.2% NH_3 (32%), B: MeOH) to give **29** as a white solid (62 mg, 0.12 mmol, 35%): ^{1}H NMR (600 MHz, [D$_6$]DMSO): δ = 7.91–7.95 (m, 2H), 7.39 (d, J = 9.4 Hz, 1H), 4.22 (q, J = 7.0 Hz, 2H), 3.84 (br s, 1H), 3.57 (br s, 2H), 3.21–3.30 (m, 3H), 3.05–3.16 (m, 4H), 2.83 (t, J = 7.3 Hz, 2H), 2.48 (s, 3H), 1.73 (sxt, J = 7.5 Hz, 2H), 1.33 (t, J = 6.8 Hz, 3H), 0.93 ppm (t, J = 7.5 Hz, 3H); ^{13}C NMR (151 MHz, [D$_6$]DMSO): δ = 160.7, 131.8, 130.1, 127.5, 114.0, 113.7, 79.4, 79.1, 78.9, 65.2, 52.0, 45.4, 40.3, 31.5, 27.3, 20.4, 14.4, 14.4, 13.9 ppm; MS (ES$^+$) *m*/*z* (%): 509 (99.7) [M^+ + H], 255 (100), 275 (99), 256 (46), 276 (37), 510 (35), 256 (20), 511 (16).

3,17β-Bis{[*tert*-butyl(dimethyl)silyl]oxy}-7α-{9-[(*R*)-(4,4,5,5,5-pentafluoropentyl)sulfinyl]nonyl}estra-1,3,5(10)-triene (31): A solution of TBSCl (1.02 g, 6.6 mmol) in DMF (5 mL) was added to a solution of imidazole (1.12 g, 16.5 mmol) in DMF (5 mL) at 0 °C. The ice bath was removed and the mixture was stirred for 10 min at RT. A solution of fulvestrant (1.00 g, 1.65 mmol) in DMF (5 mL) was added and the reaction mixture was stirred at RT overnight. The mixture was concentrated and the residue was treated with sat. aq. K_2CO_3 (10 mL) before it was extracted with CH_2Cl_2 (4×). The combined organic layer was dried (Na_2SO_4), filtered, and concentrated. The residue was purified by chromatography (hexane/EtOAc, 2:8) to give **31** as a colorless sticky oil (1.31 g, 1.57 mmol, 95%): R_f = 0.46 (hexane/EtOAc, 1:1); ^{1}H NMR (400 MHz, $CDCl_3$): δ = 7.11 (d, J = 8.4 Hz, 1H), 6.61 (dd, J = 8.4, 2.5 Hz, 1H), 6.53 (d, J = 2.5 Hz, 1H), 3.66 (t, J = 8.1 Hz, 1H), 2.79–2.89 (m, 1H), 2.58–2.79 (m, 5H), 2.10–2.35 (m, 6H), 1.88–1.99 (m, 1H), 1.84 (br d, J = 12.4 Hz, 1H), 1.67–1.80 (m, 3H), 1.10–1.66 (m, 21H), 0.98 (s, 9H), 0.89 (s, 9H), 0.74 (s, 3H), 0.19 (s, 6H), 0.04 (s, 3H), 0.03 ppm (s, 3H); ^{13}C NMR (101 MHz, $CDCl_3$): δ = 153.2, 136.8, 132.6, 126.7, 120.8, 117.1, 81.8, 52.7, 51.0, 46.1, 43.7, 41.9, 38.2, 37.4, 34.6, 33.3, 30.9, 30.0, 29.9, 29.6, 29.6, 29.4, 29.3, 29.2, 28.8, 28.2, 27.3, 25.9, 25.7, 25.6, 22.8, 22.6, 22.5, 18.1, 18.1, 14.6, 11.4, −4.4, −4.4, −4.5, −4.8 ppm.

3,17β-Bis{[*tert*-butyl(dimethyl)silyl]oxy}-7α-{9-[(*S*)-(4,4,5,5,5-pentafluoropentyl)sulfonimidoyl]nonyl}estra-1,3,5(10)-triene (32): Ammonium carbamate (16 mg, 0.20 mmol) and $PhI(OAc)_2$ (49 mg, 0.15 mmol) were added to a stirred solution of **31** (42 mg, 0.05 mmol) in MeOH (1 mL) at RT. The reaction mixture was stirred for 2 h before it was diluted with EtOAc, washed with sat. aq. $NaHCO_3$, dried (Na_2SO_4), filtered, and concentrated. The residue was purified by flash chromatography (hexane/EtOAc, 3:1) to give **32** as a colorless oil (30 mg, 0.04 mmol, 70%): R_f = 0.48 (hexane/EtOAc, 1:1); ^{1}H NMR (400 MHz, $CDCl_3$): δ = 7.11 (d, J = 8.6 Hz, 1H), 6.61 (dd, J = 8.5, 2.7 Hz, 1H), 6.53 (d, J = 2.5 Hz, 1H), 3.65 (t, J = 8.2 Hz, 1H), 2.97–3.13 (m, 4H), 2.82 (br d, J = 4.8 Hz, 1H), 2.61–2.72 (m, 1H), 2.56 (br s, 1H), 2.12–2.36 (m, 6H), 1.77–2.00 (m, 4H), 1.37–1.67 (m, 8H), 1.10–1.36 (m, 14H), 0.97 (s, 9H), 0.89 (s, 9H), 0.74 (s, 3H), 0.19 (s, 6H), 0.03 (s, 3H), 0.02 ppm (s, 3H); ^{13}C NMR (101 MHz, $CDCl_3$): δ = 153.3, 137.0, 132.7, 126.8, 120.9, 117.3, 82.0, 55.6, 53.5, 46.2, 43.8, 42.1, 38.4, 37.5, 36.8, 34.7, 33.4, 31.1, 29.8, 29.7, 29.5, 29.3, 28.4, 27.4, 26.0, 25.7, 25.8, 22.9, 22.5, 18.3, 18.3, 14.4, 11.5, −4.2, −4.2, −4.3, −4.6 ppm.

7α-{9-[(*S*)-(4,4,5,5,5-Pentafluoropentyl)sulfonimidoyl]nonyl}estra-1,3,5(10)-triene-3,17β-diol (33): A solution of TBAF in THF (1 M, 0.18 mL, 0.18 mmol) was added to a solution of **32** (30 mg, 0.04 mmol) in THF (1 mL) and the reaction mixture was stirred at 60 °C for 4 h and at RT overnight. Then, the mixture was diluted with EtOAc, washed with sat. aq. $NaHCO_3$ followed by H_2O (2×), dried (Na_2SO_4), filtered, and concentrated. The residue was purified by chromatography (hexane/EtOAc, 1:1) to afford **33** as a white solid (15 mg, 0.02 mmol, 68%): R_f = 0.36 (EtOAc); mp: 74–77 °C; ^{1}H NMR (400 MHz, $CDCl_3$): δ = 7.14 (d, J = 8.6 Hz, 1H), 6.60–6.67 (m, 1H), 6.56 (dd, J = 12.7, 2.5 Hz, 1H), 3.74 (t, J = 8.4 Hz, 1H), 2.99–3.19 (m, 4H), 2.80–2.90 (m, 1H), 2.70 (d, J = 16.5 Hz, 1H), 2.07–2.38 (m, 8H), 1.90 (d, J = 12.1 Hz, 1H), 1.77–1.87 (m, 2H), 1.73 (br d, J = 10.8 Hz, 1H), 1.54–1.68 (m, 2H), 1.12–1.51 (m, 19H), 0.96–1.07 (m, 1H), 0.78 ppm (s, 3H); ^{13}C NMR (101 MHz, $CDCl_3$): δ = 153.9, 153.6, 137.1, 137.0, 131.6, 131.4, 127.1, 116.2, 116.0, 113.0, 82.0, 55.1, 55.1, 53.6, 53.6, 46.5, 46.5, 43.4, 42.1, 42.1, 38.3, 38.3, 36.9, 34.8, 34.7, 33.3, 33.3, 30.6, 29.6, 29.3, 29.1, 29.0, 28.7, 28.6, 28.4, 27.7, 27.4, 27.3, 27.2, 27.2, 25.1, 24.9, 22.7, 22.2, 22.0, 14.3, 14.3, 14.2, 11.1 ppm; MS (ES$^+$) *m*/*z* (%): 622 (100) [M^+ + H], 623 (41), 624 (13); HRMS (ES$^+$) *m*/*z* [M^+ + H] calcd for $C_{32}H_{49}F_5NO_3S$: 622.3353, found: 622.3353.

Acknowledgements

We thank J. Geisler, R. Golde, and K. Sauvageot-Witzku for synthetic support. G. Siemeister, U. Boemer, A. Tersteegen, P. Muhn, and H. Irlbacher are acknowledged for the evaluation and discussion of in vitro pharmacology. The support of U. Ganzer and P. Lienau for the measurement and interpretation of the physicochemical and in vitro pharmacokinetic properties is highly appreciated. We thank M. Bergmann, N. Aiguabella Font, and K. Greenfield for valuable technical support with the manuscript and N. Heinrich and I. Roehr for technical support with the front cover graphic.

Conflict of interest

The authors declare no conflict of interest.

Keywords: drug design · kinase inhibitors · medicinal chemistry · pharmacophores · sulfoximines

[1] H. R. Bentley, E. E. McDermott, J. Pace, J. K. Whitehead, T. Moran, *Nature* **1949**, *163*, 675.

[2] a) C. R. Johnson, *Aldrichimica Acta* **1985**, *18*, 3; b) M. Reggelin, C. Zur, *Synthesis* **2000**, 1.

[3] a) C. R. Johnson, *Acc. Chem. Res.* **1973**, *6*, 341; b) D. Craig, F. Grellepois, A. J. P. White, *J. Org. Chem.* **2005**, *70*, 6827; c) H.-J. Gais, G. S. Babu, M. Günter, P. Das, *Eur. J. Org. Chem.* **2004**, 1464; d) M. Harmata, X. Hong, *J. Am. Chem. Soc.* **2003**, *125*, 5754; e) M. Harmata, X. Hong, C. L. Barnes, *Tetrahedron Lett.* **2003**, *44*, 7261; f) M. Harmata, N. Pavri, *Angew. Chem. Int. Ed.* **1999**, *38*, 2419; *Angew. Chem.* **1999**, *111*, 2577; g) S. Koep, H.-J. Gais, G. Raabe, *J. Am. Chem. Soc.* **2003**, *125*, 13243; h) X. Shen, W. Miao, C. Ni, J. Hu, *Angew. Chem. Int. Ed.* **2014**, *53*, 775; *Angew. Chem.* **2014**, *126*, 794; i) X. Shen, Q. Liu, W. Zhang, J. Hu, *Eur. J. Org. Chem.* **2016**, 906.

[4] a) C. Bolm, O. Simic, *J. Am. Chem. Soc.* **2001**, *123*, 3830; b) M. Harmata, S. K. Ghosh, *Org. Lett.* **2001**, *3*, 3321; c) C. Bolm, M. Martin, O. Simic, M. Verrucci, *Org. Lett.* **2003**, *5*, 427; d) C. Bolm, M. Felder, J. Müller, *Synlett* **1992**, 439; e) C. Bolm, M. Verrucci, O. Simic, P. G. Cozzi, G. Raabe, H. Okamura, *Chem. Commun.* **2003**, 2826; f) M. Langner, C. Bolm, *Angew. Chem. Int. Ed.* **2004**, *43*, 5984; *Angew. Chem.* **2004**, *116*, 6110; g) M. Langner, P. Remy, C. Bolm, *Chem. Eur. J.* **2005**, *11*, 6254; h) M. T. Reetz, O. G. Bondarev, H.-J. Gais, C. Bolm, *Tetrahedron Lett.* **2005**, *46*, 5643.

[5] G. Satzinger, *Drug News Perspect.* **2001**, *14*, 197.

[6] U. Lücking, *Angew. Chem. Int. Ed.* **2013**, *52*, 9399; *Angew. Chem.* **2013**, *125*, 9570.

[7] a) T. C. Sparks, G. B. Watson, M. R. Loso, C. Geng, J. M. Babcock, J. D. Thomas, *Pestic. Biochem. Physiol.* **2013**, *107*, 1; b) K. E. Arndt, D. C. Bland, N. M. Irvine, S. L. Powers, T. P. Martin, J. R. McConnell, D. E. Podhorez, J. M. Renga, R. Ross, G. A. Roth, B. D. Scherzer, T. W. Toyzan, *Org. Process Res. Dev.* **2015**, *19*, 454.

[8] a) G. Satzinger, P. Stoss, *Arzneim.-Forsch.* **1970**, *20*, 1214; b) R. D. Dillard, T. T. Yen, P. Stark, D. E. Parvey, *J. Med. Chem.* **1980**, *23*, 717; c) H. Ikeuchi, Y.-M. Ahn, T. Otokawa, B. Watanabe, L. Hegazy, J. Hiratake, N. G. J. Richards, *Bioorg. Med. Chem.* **2012**, *20*, 5915.

[9] a) H. Okamura, C. Bolm, *Org. Lett.* **2004**, *6*, 1305; b) Y. Cho, C. Bolm, *Tetrahedron Lett.* **2005**, *46*, 8007; c) O. García Mancheño, C. Bolm, *Org. Lett.* **2007**, *9*, 2951; d) A. Pandey, C. Bolm, *Synthesis* **2010**, 2922; e) J. Gries, J. Krüger, *Synlett* **2014**, *25*, 1831; f) H. Lebel, H. Piras, J. Bartholomeüs, *Angew. Chem. Int. Ed.* **2014**, *53*, 7300; *Angew. Chem.* **2014**, *126*, 7428; g) J. Miao, N. G. J. Richards, H. Ge, *Chem. Commun.* **2014**, *50*, 9687; h) C. A. Dannenberg, V. Bizet, C. Bolm, *Synthesis* **2015**, *47*, 1951; i) V. Bizet, C. M. M. Hendriks, C. Bolm, *Chem. Soc. Rev.* **2015**, *44*, 3378; j) M. Zenzola, R. Doran, R. Luisi, J. A. Bull, *J. Org. Chem.* **2015**, *80*, 6391.

[10] a) B. Gutmann, P. Elsner, A. O'Kearney-McMullan, W. Goundry, D. M. Roberge, C. O. Kappe, *Org. Process Res. Dev.* **2015**, *19*, 1062; b) H. Lebel, H. Piras, M. Borduy, *ACS Catal.* **2016**, *6*, 1109.

[11] J. A. Sirvent, D. Bierer, R. Webster, U. Lücking, *Synthesis* **2017**, *49*, 1024.

[12] A. Tota, M. Zenzola, S. J. Chawner, S. St John-Campbell, C. Carlucci, G. Romanazzi, L. Degennaro, J. A. Bull, R. Luisi, *Chem. Commun.* **2017**, *53*, 348.

[13] a) Y. Zhu, M. R. Loso, G. B. Watson, T. C. Sparks, R. B. Rogers, J. X. Huang, B. C. Gerwick, J. M. Babcock, D. Kelley, V. B. Hedge, B. M. Nugent, J. M. Renga, I. Denholm, K. Gorman, G. J. DeBoer, J. Hasler, T. Meade, J. D. Thomas, *J. Agric. Food Chem.* **2011**, *59*, 2950; b) U. Lücking, R. Jautelat, M. Krüger, T. Brumby, P. Lienau, M. Schäfer, H. Briem, J. Schulze, A. Hillisch, A. Reichel, A. M. Wengner, G. Siemeister, *ChemMedChem* **2013**, *8*, 1067; c) F. W. Goldberg, J. G. Kettle, J. Xiong, D. Lin, *Tetrahedron* **2014**, *70*, 6613; d) F. W. Goldberg, J. G. Kettle, T. Kogej, M. W. D. Perry, N. P. Tomkinson, *Drug Discovery Today* **2015**, *20*, 11; e) N. Nishimura, M. H. Norman, L. Liu, K. C. Yang, K. S. Ashton, M. D. Bartberger, S. Chmait, J. Chen, R. Cupples, C. Fotsch, J. Helmering, S. R. Jordan, R. K. Kunz, L. D. Pennington, S. F. Poon, A. Siegmund, G. Sivits, D. J. Lloyd, C. Hale, D. J. St. Jean, Jr., *J. Med. Chem.* **2014**, *57*, 3094; f) S. Boral, S. Wang, T. Malon, J. Wurster, J. Shen, M. Robinson (Allergan, Inc.), US Pat. No. 20150166521, **2015**; g) A. Blum (Boehringer Ingelheim), Int. PCT Pub. No. WO2015169677, **2015**; h) T. Johnson, R. Vairagoundar, R. A. Ewin (Zoetis LLC), Int. PCT Pub. No. WO2014172443, **2014**; i) B. M. Nugent, A. M. Buysse, M. R. Loso, J. M. Babcock, T. C. Johnson, M. P. Oliver, T. P. Martin, M. S. Ober, N. Breaux, A. Robinson, Y. Adelfinskaya, *Pest Manage. Sci.* **2015**, *71*, 928; j) F. von Nussbaum, V. M.-J. Li, S. Allerheiligen, S. Anlauf, L. Bärfacker, M. Bechem, M. Delbeck, M. F. Fitzgerald, M. Gerisch, H. Gielen-Haertwig, H. Haning, D. Karthaus, D. Lang, K. Lustig, D. Meibom, J. Mittendorf, U. Rosentreter, M. Schäfer, S. Schäfer, J. Schamberger, L. A. Telan, A. Tersteegen, *ChemMedChem* **2015**, *10*, 1163; k) Also see ref. 6 and references therein.

[14] G. Siemeister, U. Luecking, A. M. Wengner, P. Lienau, W. Steinke, C. Schatz, D. Mumberg, K. Ziegelbauer, *Mol. Cancer Ther.* **2012**, *11*, 2265.

[15] a) A. Scholz, T. Oellerich, A. Hussain, S. Lindner, U. Luecking, A. O. Walter, P. Ellinghaus, R. Valencia, F. von Nussbaum, D. Mumberg, M. Brands, S. Ince, H. Serve, K. Ziegelbauer, *Cancer Res.* **2016**, *76 (Suppl. 14)*, DOI: 10.1158/1538-7445.AM2016-3022; b) A. Scholz, U. Luecking, G. Siemeister, P. Lienau, U. Boemer, P. Ellinghaus, A. O. Walter, R. Valencia, S. Ince, F. von Nussbaum, D. Mumberg, M. Brands, K. Ziegelbauer, *Cancer Res.* **2015**, *75 (Suppl. 15)*, DOI: 10.1158/1538-7445.AM2015-DDT02-02; c) U. Luecking, A. Scholz, P. Lienau, G. Siemeister, D. Kosemund, R. Bohlmann, K. Eis, M. Gnoth, I. Terebesi, K. Meyer, K. Prelle, R. Valencia, S. Ince, F. von Nussbaum, D. Mumberg, K. Ziegelbauer, B. Klebl, A. Choidas, P. Nussbaumer, M. Baumann, C. Schultz-Fademrecht, G. Ruehter, J. Eickhoff, M. Brands, *Cancer Res.* **2015**, *75 (Suppl. 15)*, DOI: 10.1158/1538-7445.AM2015-2828.

[16] K. M. Foote, A. Lau, J. W. M. Nissink, *Future Med. Chem.* **2015**, *7*, 873.

[17] M. Frings, C. Bolm, A. Blum, C. Gnamm, *Eur. J. Med. Chem.* **2017**, *126*, 225.

[18] a) U. Lücking, M. Krueger, R. Jautelat, G. Siemeister (Schering AG), Int. PCT Pub. No. WO2005037800, **2005**; b) U. Lücking, G. Siemeister, R. Jautelat (Schering Aktiengesellschaft), Int. PCT Pub. No. WO2006099974, **2006**; c) U. Lücking (Schering Aktiengesellschaft), Eur. Pat. No. EP1710246, **2006**; d) U. Lücking, G. Kettschau, H. Briem, W. Schwede, M. Schäfer, K.-H. Thierauch, M. Husemann (Schering Aktiengesellschaft), Int. PCT Pub. No. WO2006108695, **2006**; e) U. Luecking, D. Nguyen, A. von Bonin, O. von Ahsen, M. Krueger, H. Briem, G. Kettschau, O. Prien, A. Mengel, K. Krolikiewicz, U. Boemer, U. Bothe, I. Hartung (Schering Aktiengesellschaft), Int. PCT Pub. No. WO2007071455, **2007**; f) U. Lücking, G. Siemeister, B. Bader (Schering Aktiengesellschaft), Int. PCT Pub. No. WO2007079982, **2007**; g) U. Luecking, G. Siemeister, R. Jautelat (Bayer Schering Pharma Aktiengesellschaft), Int. PCT Pub. No. WO2008025556, **2008**; h) O. Prien, K. Eis, U. Lücking, J. Guenther, D. Zopf (Bayer Schering Pharma Aktiengesellschaft), Ger. Pat. No. DE102007024470, **2008**; i) I. Hartung, U. Bothe, G. Kettschau, U. Luecking, A. Mengel, M. Krueger, K.-H. Thierauch, P. Lienau, U. Boemer (Bayer Schering Pharma Aktiengesellschaft), Int. PCT Pub. No. WO2008155140, **2008**; j) D. Nguyen, A. Von Bonin, M. Haerter, H. Schirok, A. Mengel, O. Von Ahsen (Bayer Schering Pharma Aktiengesellschaft), Int. PCT Pub. No. WO2009089851, **2009**; k) M. Härter, H. Beck, P. Ellinghaus, K. Berhoerster, S. Greschat, K.-H. Thierauch, F. Süssmeier (Bayer Schering Pharma Aktiengesellschaft), Int. PCT Pub. No. WO2010054763, **2010**; l) F. von Nussbaum, D. Karthaus, S. Anlauf, M. Delbeck, V. M.-J. Li, D. Meibom, K. Lustig, D. Schneider (Bayer

Schering Pharma Aktiengesellschaft), Int. PCT Pub. No. WO2010115548, **2010**; m) W. Schwede, U. Klar, C. Möller, A. Rotgeri, W. Bone (Bayer Schering Pharma Aktiengesellschaft), Int. PCT Pub. No. WO2011009531, **2011**; n) U. Lücking, A. Cleve, B. Haendler, H. Faus, S. Köhr, H. Irlbacher (Bayer Schering Pharma Aktiengesellschaft), Int. PCT Pub. No. WO2011029537, **2011**; o) U. Lücking, R. Bohlmann, A. Scholz, G. Siemeister, M. J. Gnoth, U. Boemer, D. Kosemund, P. Lienau, G. Ruether, C. Schulz-Fademrecht (Bayer Intellectual Property GmbH), Int. PCT Pub. No. WO2012160034, **2012**.

[19] a) D. G. Savage, K. H. Antman, *N. Engl. J. Med.* **2002**, *346*, 683; b) M. Beran, X. Cao, Z. Estrov, S. Jeha, G. Jin, S. O'Brien, M. Talpaz, R. B. Arlinghaus, N. B. Lydon, H. Kantarjian, *Clin. Cancer Res.* **1998**, *4*, 1661; c) E. Buchdunger, C. L. Cioffi, N. Law, D. Stover, S. Ohno-Jones, B. J. Druker, N. B. Lydon, *J. Pharmacol. Exp. Ther.* **2000**, *295*, 139.

[20] R. Capdeville, E. Buchdunger, J. Zimmermann, A. Matter, *Nat. Rev. Drug Discovery* **2002**, *1*, 493.

[21] a) Y.-L. Lin, Y. Meng, W. Jiang, B. Roux, *Proc. Natl. Acad. Sci. USA* **2013**, *110*, 1664; b) A. Aleksandrov, T. Simonson, *J. Comput. Chem.* **2010**, *31*, 1551.

[22] B. Peng, P. Lloyd, H. Schran, *Clin. Pharmacokinet.* **2005**, *44*, 879.

[23] M. Michaelides, D. H. Albert in *Kinase Inhibitor Drugs* (Eds.: R. Li, J. A. Stafford), Wiley, Hoboken, **2009**, pp. 79 – 112.

[24] D. T. Manallack, R. J. Prankerd, E. Yuriev, T. I. Oprea, D. K. Chalmers, *Chem. Soc. Rev.* **2013**, *42*, 485.

[25] For a review on piperazines in drug discovery, see: R. V. Patel, S. W. Park, *Mini-Rev. Med. Chem.* **2013**, *13*, 1579.

[26] B. A. Müller, *Curr. Pharm. Des.* **2009**, *15*, 120.

[27] M. I. Davis, J. P. Hunt, S. Herrgard, P. Ciceri, L. M. Wodicka, G. Pallares, M. Hocker, D. K. Treiber, P. P. Zarrinkar, *Nat. Biotechnol.* **2011**, *29*, 1046.

[28] For the assay description, see: T. Onofrey, G. Kazan, Millipore Corporation Application Note AN1731EN00, **2003**.

[29] For the assay description, see: D. J. Minick, J. H. Frenz, M. A. Patrick, D. A. Brent, *J. Med. Chem.* **1988**, *31*, 1023.

[30] For the assay description, see: U. Lücking, P. Wasnaire, A. Scholz, P. Lienau, G. Siemeister, C. Stegmann, U. Boemer, K. Zheng, P. Gao, G. Chen, J. Xi (Bayer Pharma Aktiengesellschaft), Int. PCT Pub. No. WO2015155197, **2015**.

[31] See, for example: G. M. Rishton, *Drug Discovery Today* **2003**, *8*, 86.

[32] C. A. Lipinski, F. Lombardo, B. W. Dominy, P. J. Feeney, *Adv. Drug Delivery Rev.* **2001**, *46*, 3.

[33] P. Wu, T. E. Nielsen, M. H. Clausen, *Drug Discovery Today* **2016**, *21*, 5.

[34] J. Wesierska-Gadek, I. Chamrad, V. Krystof, *Future Med. Chem.* **2009**, *1*, 1561.

[35] L. Santo, S. Vallet, T. Hideshima, D. Cirstea, H. Ikeda, S. Pozzi, K. Patel, Y. Okawa, G. Gorgun, G. Perrone, E. Calabrese, M. Yule, M. Squires, M. Ladetto, M. Boccadoro, P. G. Richardson, N. C. Munshi, K. C. Anderson, N. Raje, *Oncogene* **2010**, *29*, 2325.

[36] E. X. Chen, S. Hotte, H. Hirte, L. L. Siu, J. Lyons, M. Squires, S. Lovell, S. Turner, L. McIntosh, L. Seymour, *Br. J. Cancer* **2014**, *111*, 2262.

[37] P. G. Wyatt, A. J. Woodhead, V. Berdin, J. A. Boulstridge, M. G. Carr, D. M. Cross, D. J. Davis, L. A. Devine, T. R. Early, R. E. Feltell, E. J. Lewis, R. L. McMenamin, E. F. Navarro, M. A. O'Brien, M. O'Reilly, M. Reule, G. Saxty, L. C. A. Seavers, D.-M. Smith, M. S. Squires, G. Trewartha, M. T. Walker, A. J.-A. Woolford, *J. Med. Chem.* **2008**, *51*, 4986.

[38] See, for example: E. H. Kerns, L. Di, *Drug-like Properties: Concepts, Structure Design and Methods*, Academic Press, Burlington, **2008**, pp. 276 – 286.

[39] For the assay description, see: U. Lücking, N. Böhnke, A. Scholz, P. Lienau, G. Siemeister, U. Bömer, D. Kosemund, R. Bohlmann (Bayer Schering Pharma Aktiengesellschaft), Int. PCT Pub. No. WO2014076091, **2014**.

[40] U. Asghar, A. K. Witkiewicz, N. C. Turner, E. S. Knudsen, *Nat. Rev. Drug Discovery* **2015**, *14*, 130.

[41] B. O'Leary, R. S. Finn, N. C. Turner, *Nat. Rev. Clin. Oncol.* **2016**, *13*, 417.

[42] a) P. L. Toogood, P. J. Harvey, J. T. Repine, D. J. Sheehan, S. N. VanderWel, H. R. Zhou, P. R. Keller, D. J. McNamara, D. Sherry, T. Zhu, J. Brodfuehrer, C. Choi, M. R. Barvian, D. W. Fry, *J. Med. Chem.* **2005**, *48*, 2388; b) H. Lu, U. Schulze-Gahmen, *J. Med. Chem.* **2006**, *49*, 3826; c) P. L. Toogood, N. D. Ide in *Innovative Drug Synthesis*, 1st ed. (Eds.: J. J. Li, D. S. Johnson), Wiley, **2016**, pp. 167 – 195.

[43] S. Kim, A. Loo, R. Chopra, G. Caponigro, A. Huang, S. Vora, S. Parasuraman, S. Howard, N. Keen, W. Sellers, C. Brain, *Mol. Cancer Ther.* **2013**, *12 (Suppl. 11)*, PR02.

[44] L. M. Gelbert, S. Cai, X. Lin, C. Sanchez-Martinez, M. del Prado, M. J. Lallena, R. Torres, R. T. Ajamie, G. N. Wishart, R. S. Flack, B. L. Neubauer, J. Young, E. M. Chan, P. Iversen, D. Cronier, E. Kreklau, A. de Dios, *Invest. New Drugs* **2014**, *32*, 825.

[45] a) For a recent study of palbociclib analogues modified at the terminal piperazine ring, see: P. Wang, J. Huang, K. Wang, Y. Gu, *Eur. J. Med. Chem.* **2016**, *122*, 546.

[46] a) J. D. Corbin, S. H. Francis, *J. Biol. Chem.* **1999**, *274*, 13729; b) J. D. Corbin, S. H. Francis, D. J. Webb, *Urology* **2002**, *60*, 4.

[47] P. Sandner, N. Svenstrup, H. Tinel, H. Haning, E. Bischoff, *Expert Opin. Ther. Pat.* **2008**, *18*, 21.

[48] Z. Sui, *Expert Opin. Ther. Pat.* **2003**, *13*, 1373.

[49] B. Sung, K. Y. Hwang, Y. H. Jeon, J. I. Lee, Y.-S. Heo, J. H. Kim, J. Moon, J. M. Yoon, Y.-L. Hyun, E. Kim, S. J. Eum, S.-Y. Park, J.-O. Lee, T. G. Lee, S. Ro, J. M. Cho, *Nature* **2003**, *425*, 98.

[50] a) J. D. Corbin, A. Beasley, M. A. Blount, S. H. Francis, *Neurochem. Int.* **2004**, *45*, 859; b) H. Haning, U. Niewöhner, T. Schenke, T. Lampe, A. Hillisch, E. Bischoff, *Bioorg. Med. Chem. Lett.* **2005**, *15*, 3900.

[51] For the assay description, see: F. Wunder, A. Tersteegen, A. Rebmann, C. Erb, T. Fahrig, M. Hendrix, *Mol. Pharmacol.* **2005**, *68*, 1775.

[52] D. F. Veber, S. R. Johnson, H. Y. Cheng, B. R. Smith, K. W. Ward, K. D. Kopple, *J. Med. Chem.* **2002**, *45*, 2615.

[53] E. Ciruelos, T. Pascual, M. L. Arroyo Vozmediano, M. Blanco, L. Manso, L. Parrilla, C. Muñoz, E. Vega, M. J. Calderón, B. Sancho, H. Cortes-Funes, *Breast* **2014**, *23*, 201.

[54] J. R. Evans, R. U. Grundy (Astra Zeneca), Int. PCT Pub. No. WO200151056, **2001**.

[55] M. Harrison, A. Laight, D. Clarke, P. Giles, R. Yates, *Eur. J. Cancer* **2003**, *1 (Suppl. 5)*, S171.

[56] J. F. R. Robertson, M. Harrison, *Br. J. Cancer* **2004**, *90*, S7.

[57] M. Zenzola, R. Doran, L. Degennaro, R. Luisi, J. A. Bull, *Angew. Chem. Int. Ed.* **2016**, *55*, 7203; *Angew. Chem.* **2016**, *128*, 7319.

[58] For the assay description, see: L. Zorn, D. Kosemund, C. Möller, H. Irlbacher, R. Nubbemeyer, A. Ter Laak, U. Bothe (Bayer Pharma Aktiengesellschaft), Int. PCT Pub. No. WO2015028409, **2015**.

[59] For the assay description, see: J. Hoffmann, R. Bohlmann, N. Heinrich, H. Hofmeister, J. Kroll, H. Künzer, R. B. Lichtner, Y. Nishino, K. Parczyk, G. Sauer, H. Gieschen, H.-F. Ulbrich, M. R. Schneider, *J. Natl. Cancer Inst.* **2004**, *96*, 210.

Manuscript received: January 23, 2017

Accepted Article published: February 21, 2017

Final Article published: March 22, 2017

